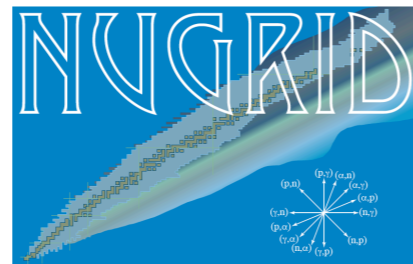


Low- and intermediate mass stellar evolution and recurrent H-ingestion events in super-AGB thermal pulses



Marco Pignatari (Basel)



Bill Paxton (KITP)



Paul Woodward (U Minnesota)



Sam Jones, Michael Bennett (Keele)

Falk Herwig

Dept. of Physics and Astronomy
University of Victoria



Nuclear astrophysics and near-field cosmology

- understanding SFH and chemical evolution in dSph galaxies
- constrain nucleosynthesis processes, e.g. Eu vs α -elements
- near-field cosmology: identify the building blocks of our galaxy

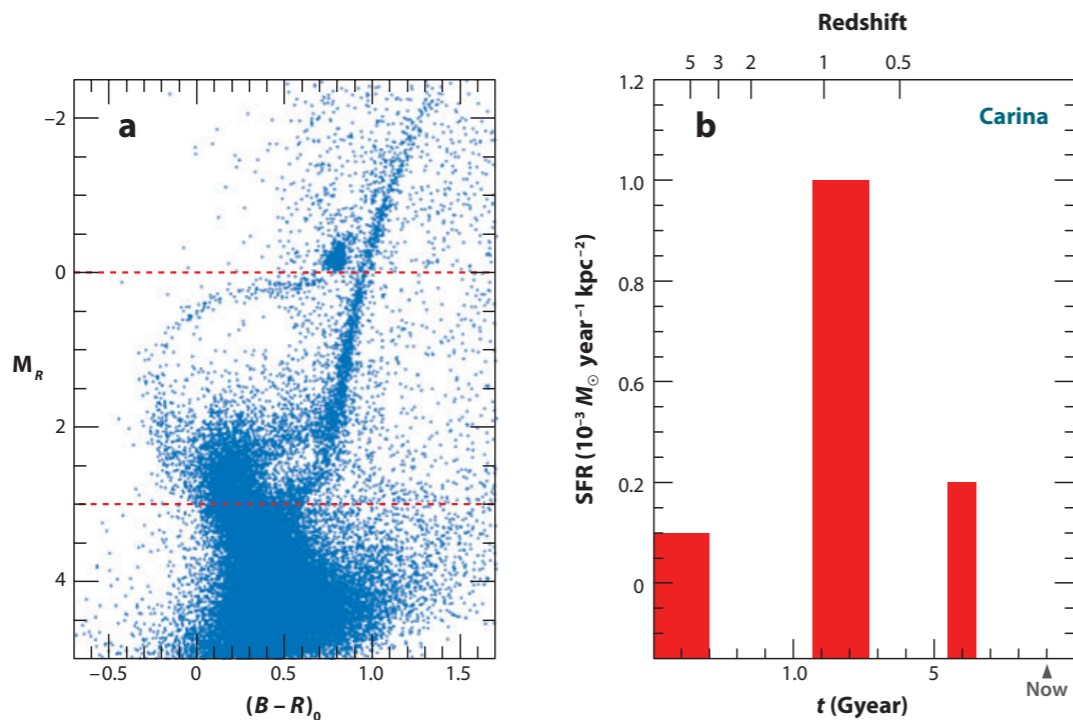
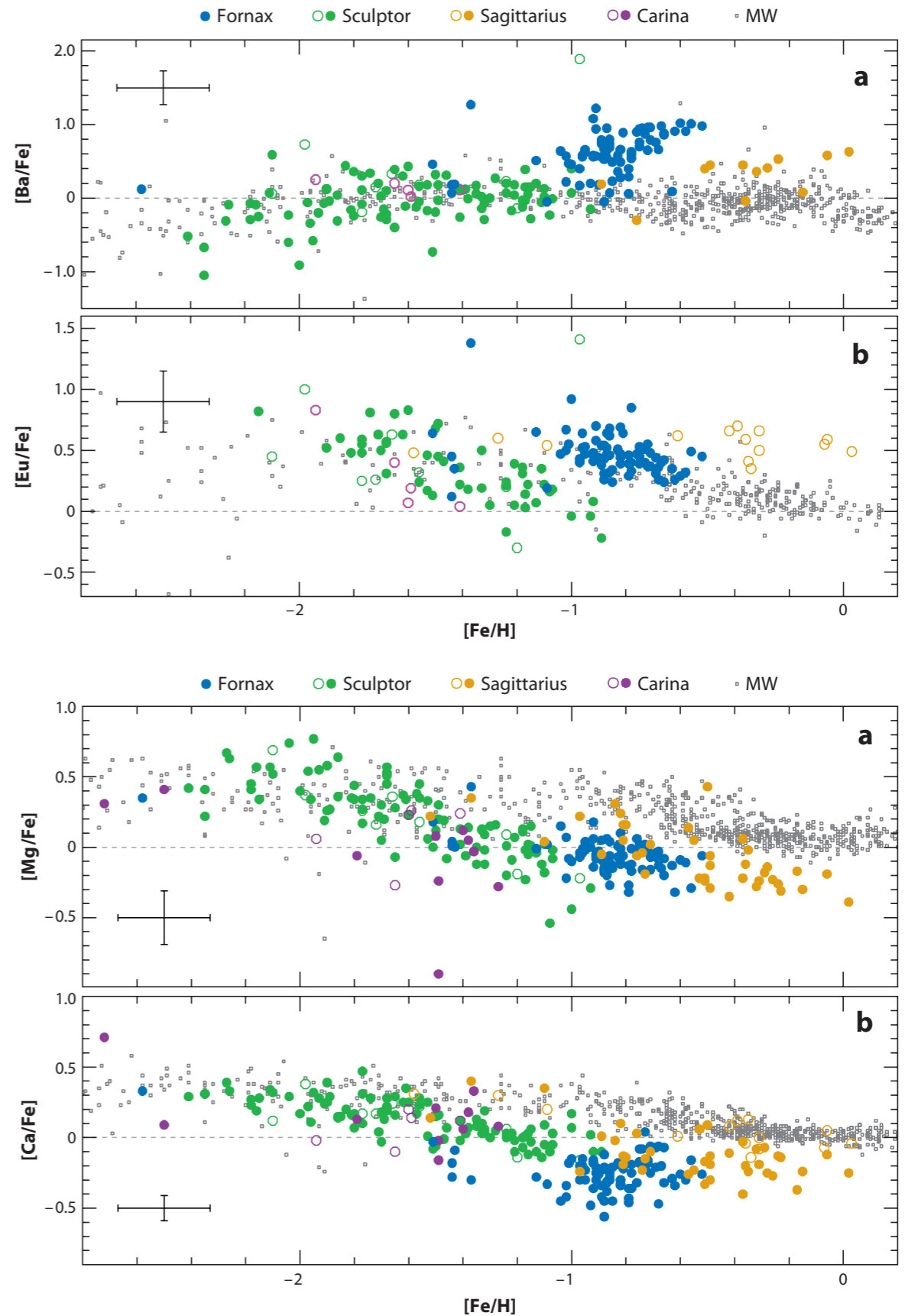


Figure 4

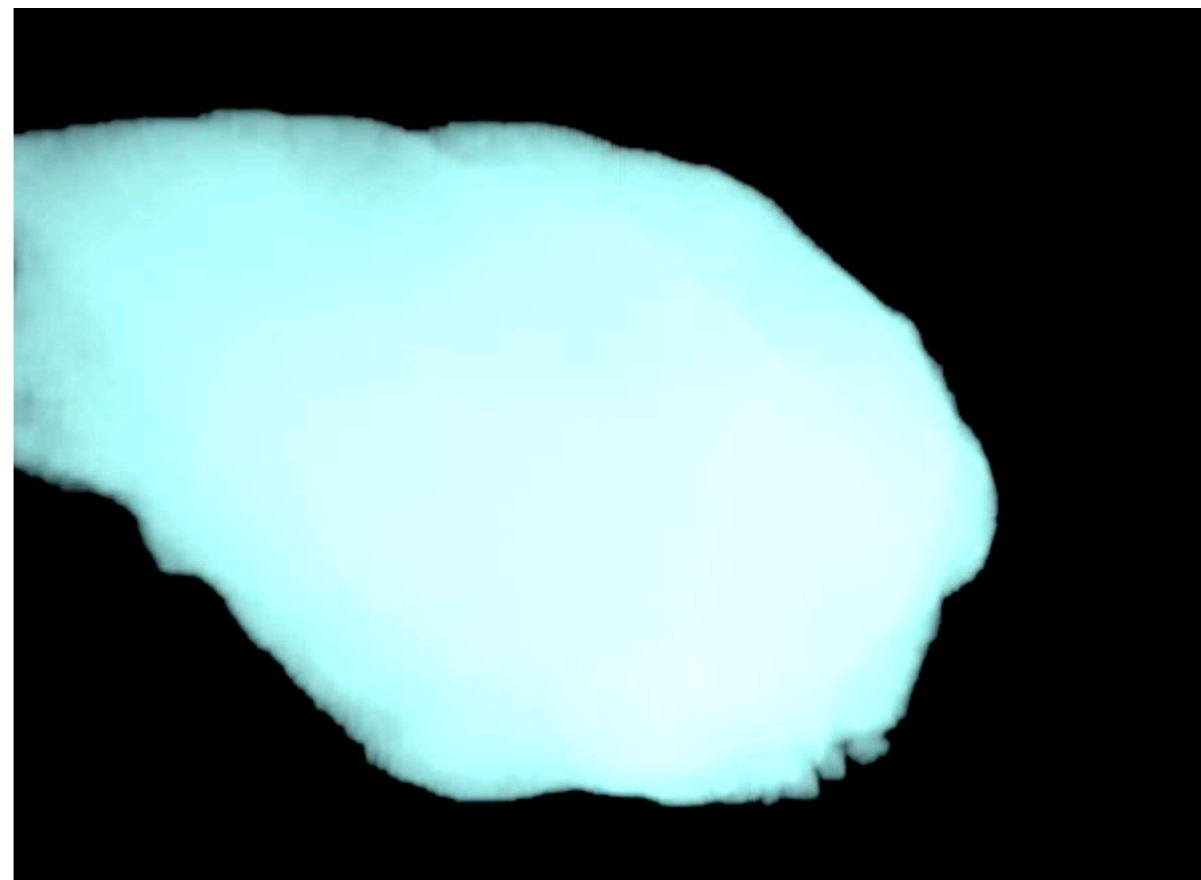
(a) A color-magnitude diagram of the Carina dwarf spheroidal (obtained by M. Mateo with the CTIO 4-m and MOSAIC camera, private communication) in the central 30' of the galaxy. This clearly shows the presence of at least three distinct MSTOs. (b) The star-formation history of the central region of Carina determined by Hurley-Keller, Mateo & Nemeč (1998), showing the relative strength of the different bursts. The ages are also shown in terms of redshift.



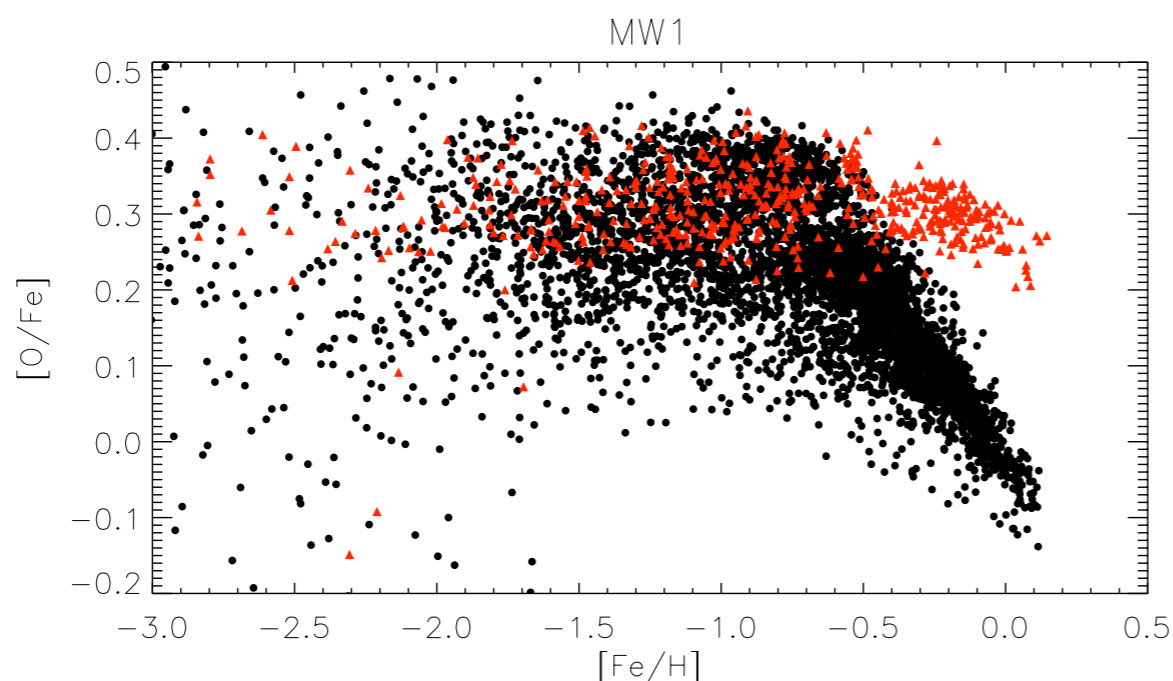
Tolstoy et al 2009 (ARAA)

The hierarchy of GCE simulation types

- analytic models, incl. one or a few zones, parameterized everything (e.g. Matteucci, Timmes, Travaglio, and many more)
- semi-analytical models, amounts to a post-processing along a cosmological merger-tree from simulations (e.g. Font et al., Tumlinson and collaborators, and many more)
- cosmological simulations with multiple tracer fields (e.g. Kobayashi, Zolotov et al. 2010)

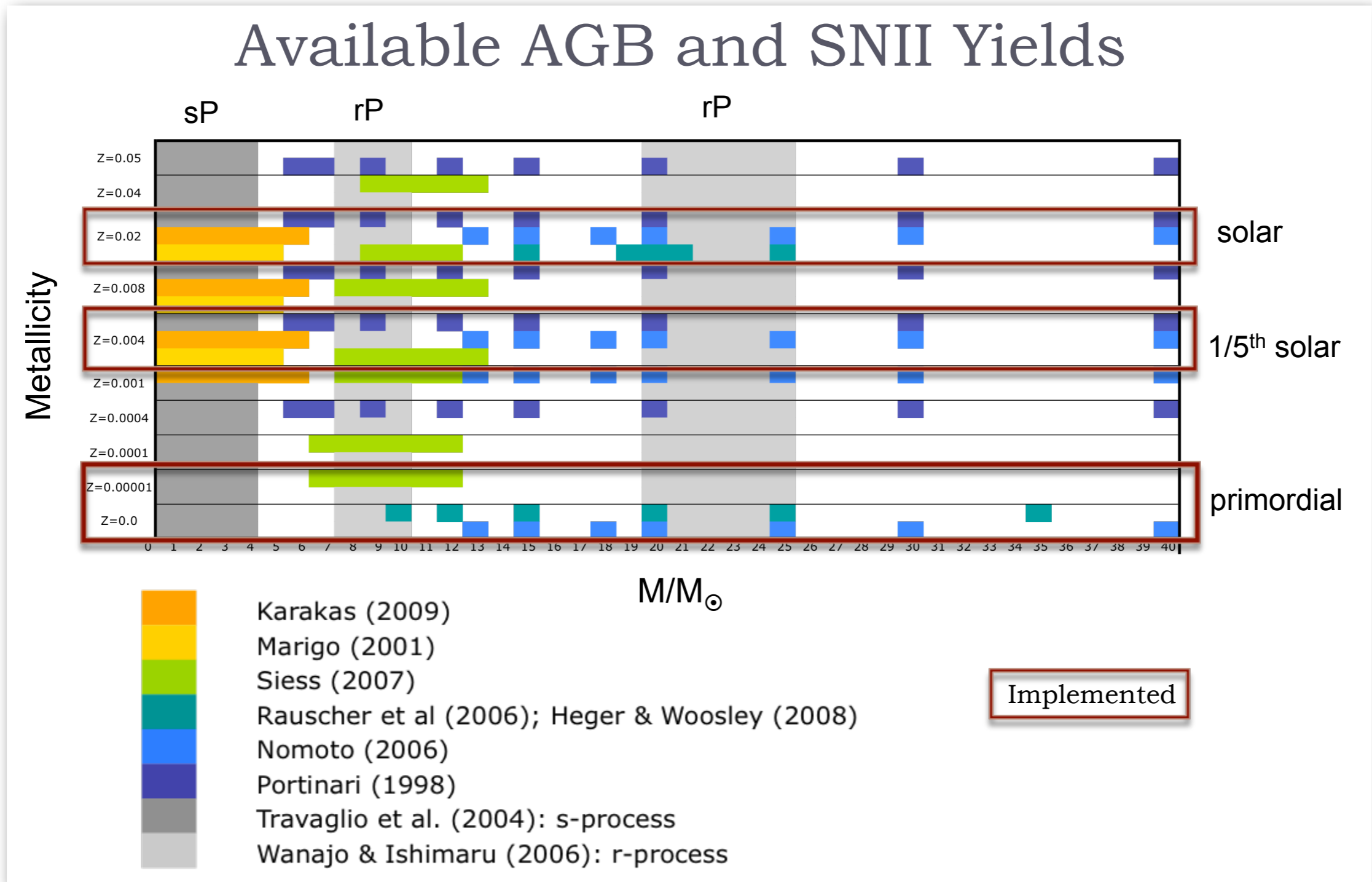


Fabio Governato, U Washington, Seattle

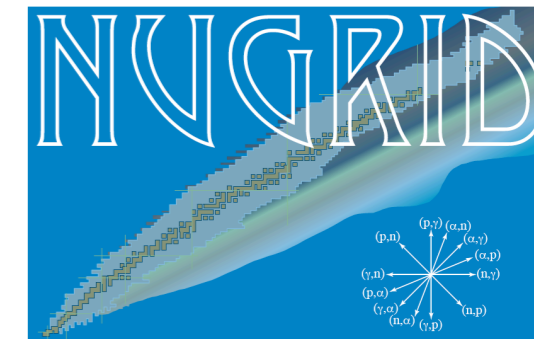


“observed” halo stars in a cosmological high-resolution disc galaxy simulation, separating out in-situ stars (**red triangles**) and accreted stars (**black dots**)

For all these applications an internally consistent simulation data set of yields is needed



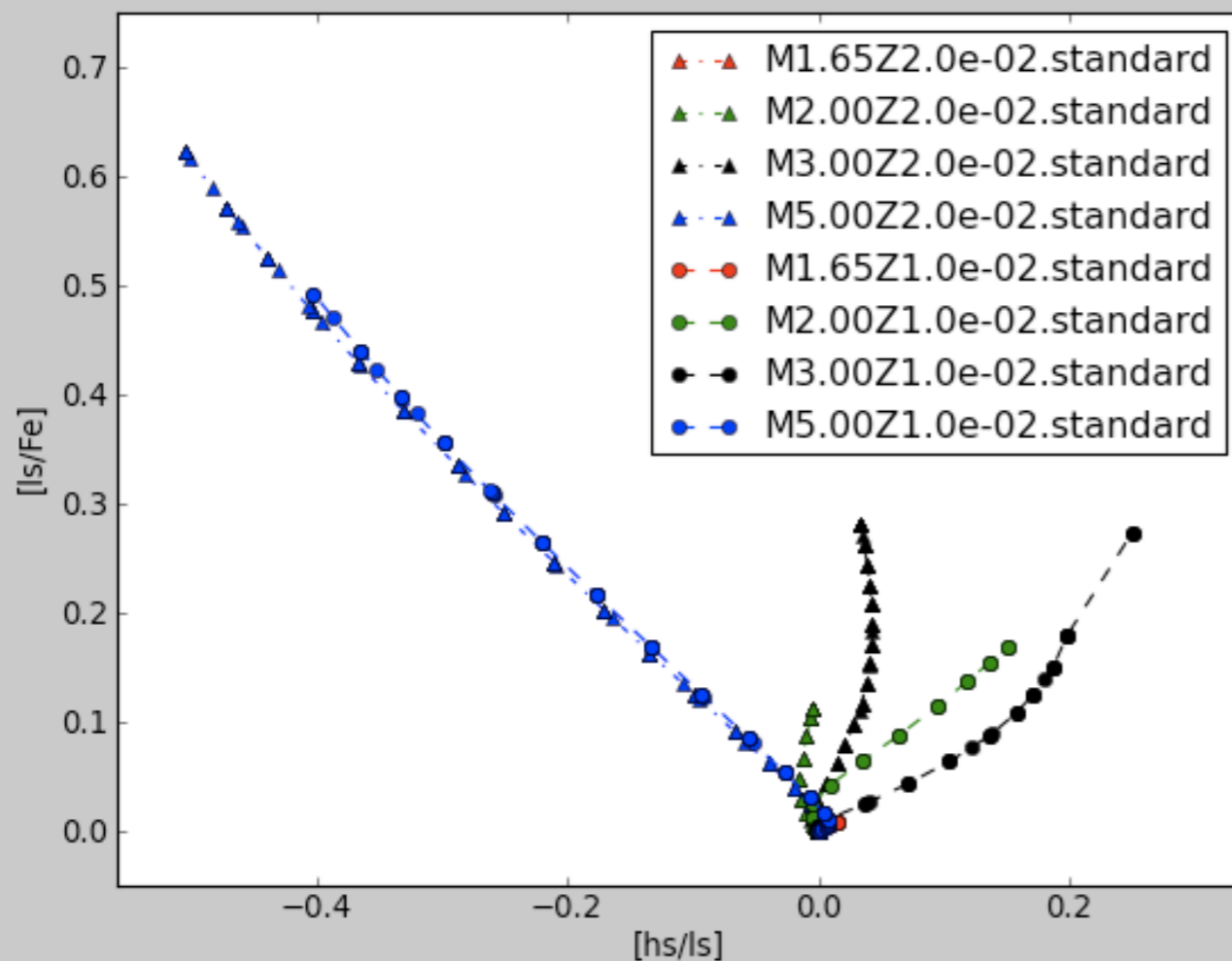
overall s-process indices in AGB stars



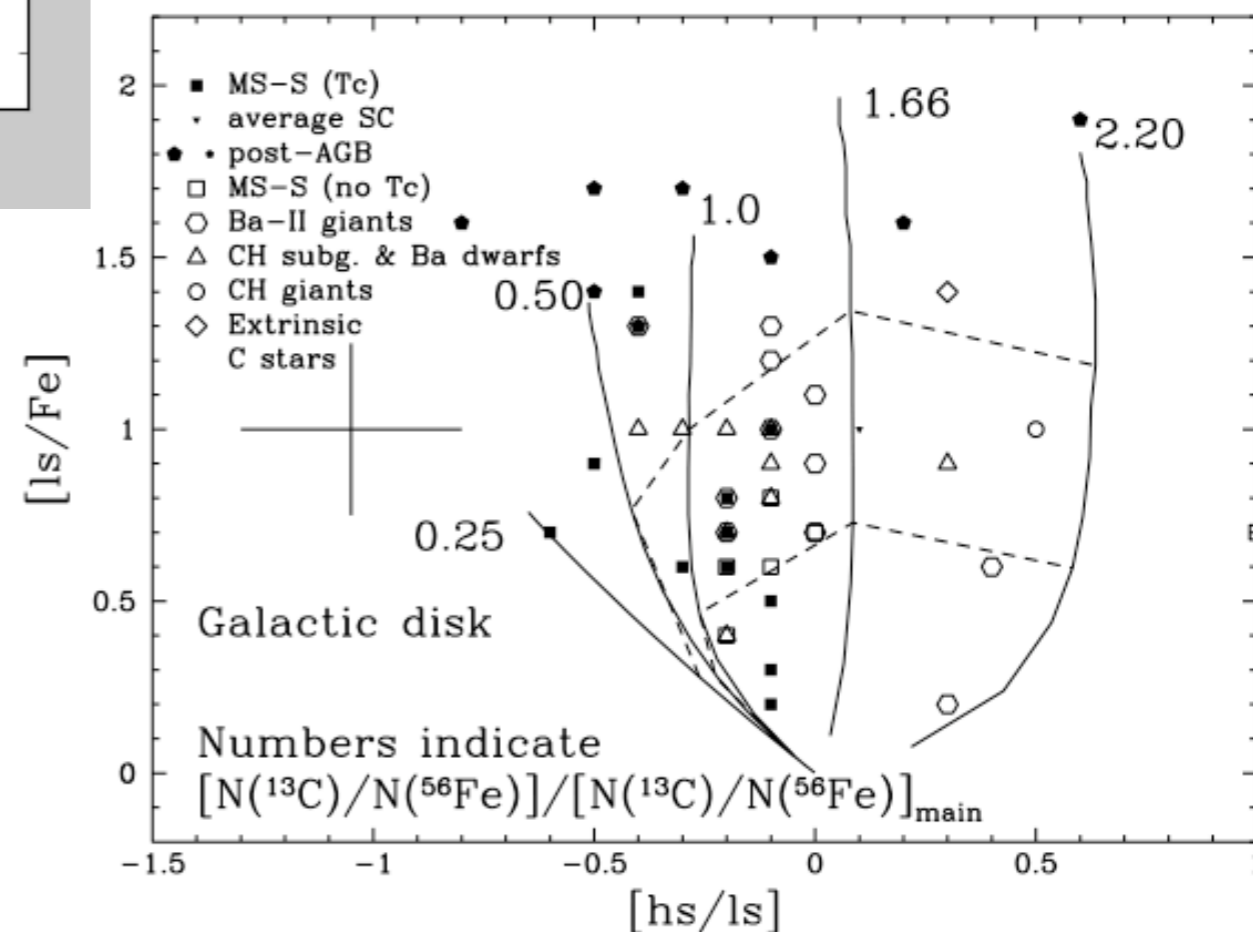
NuGrid: Set I

hs: $\langle \text{Ba, La, Ce, Nd, La, Sm} \rangle$

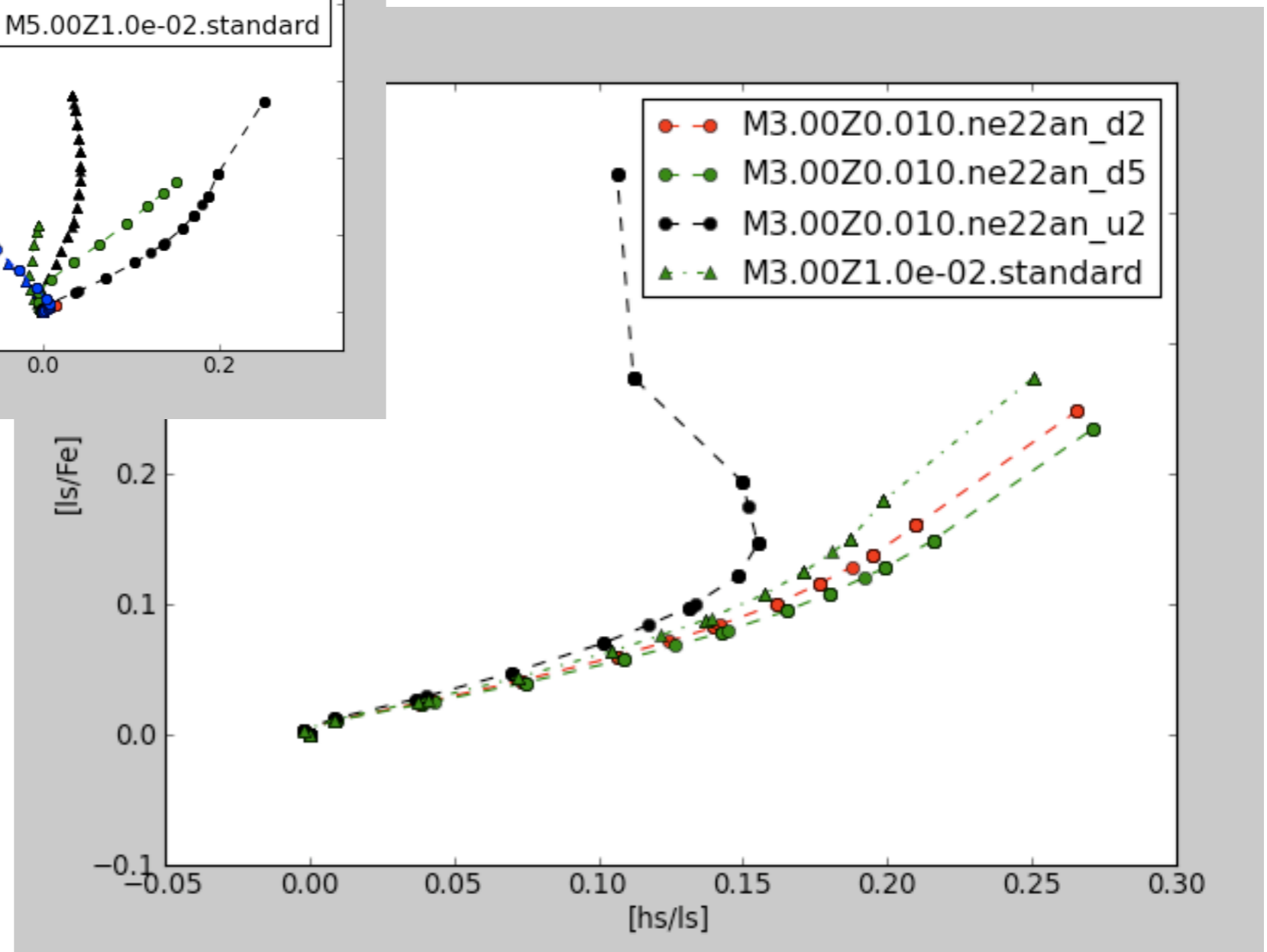
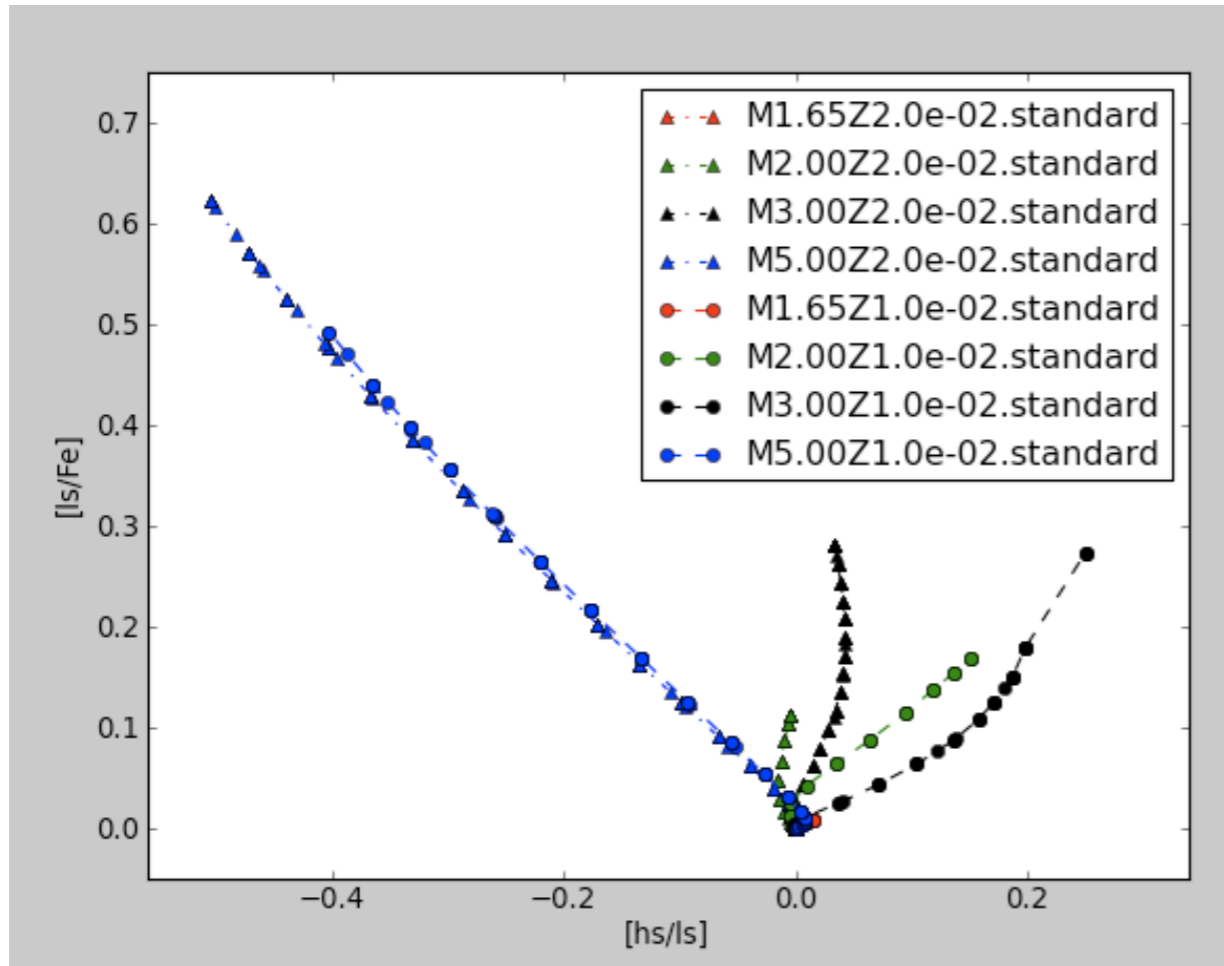
ls: $\langle \text{Y, Zr} \rangle$



observations and parameterized models (Busso et al 2001)



$^{22}\text{Ne}(\alpha,n)$ reaction rate uncertainty impact



Branching at ^{95}Zr in AGB stars

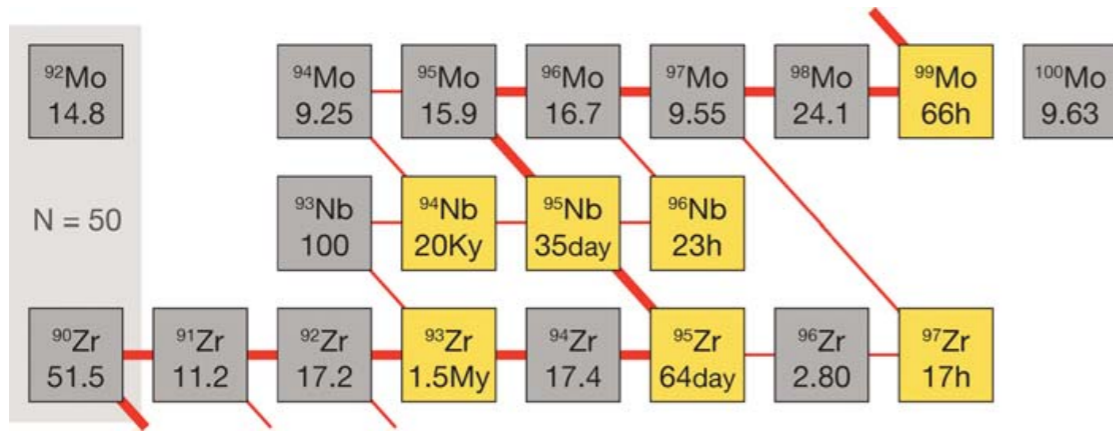
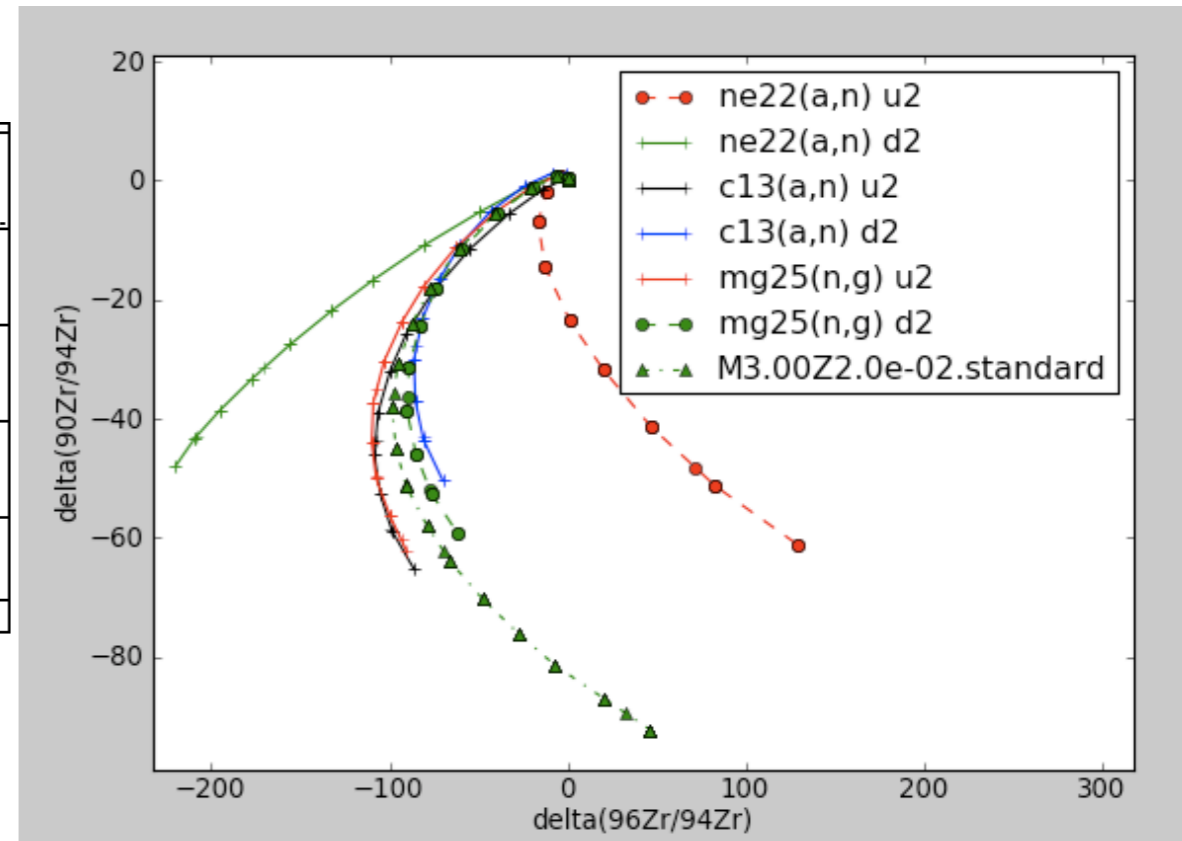
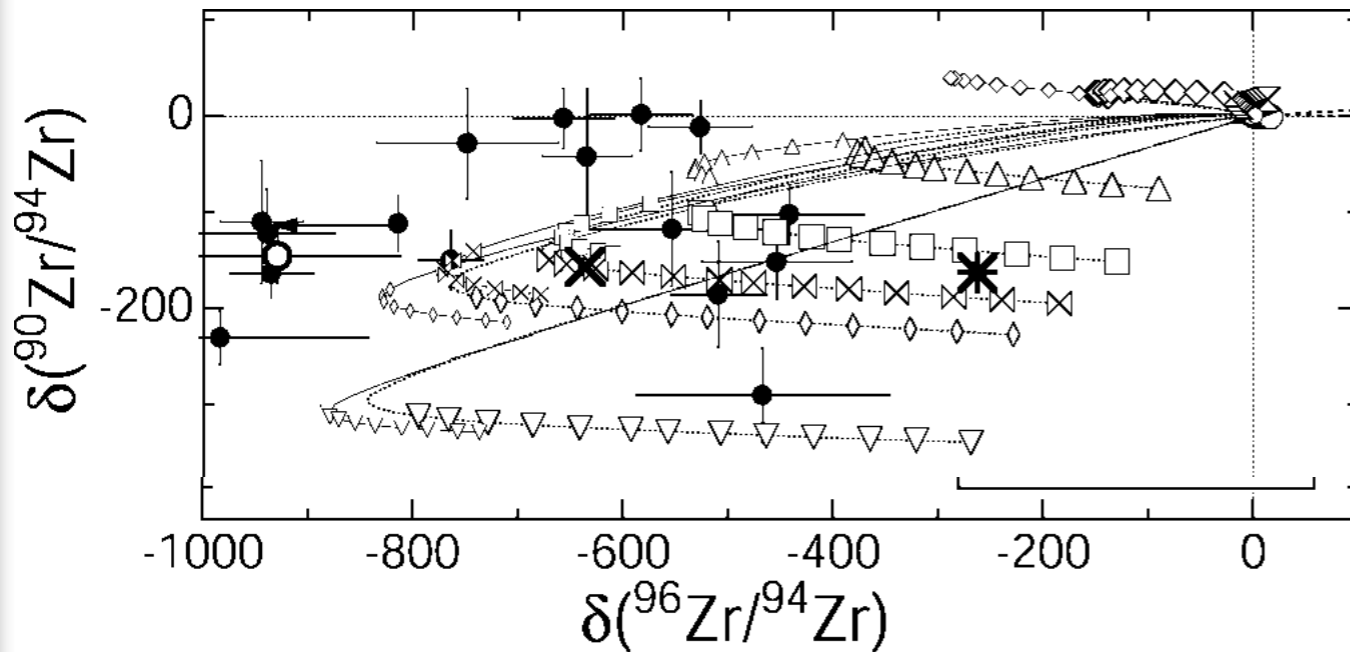
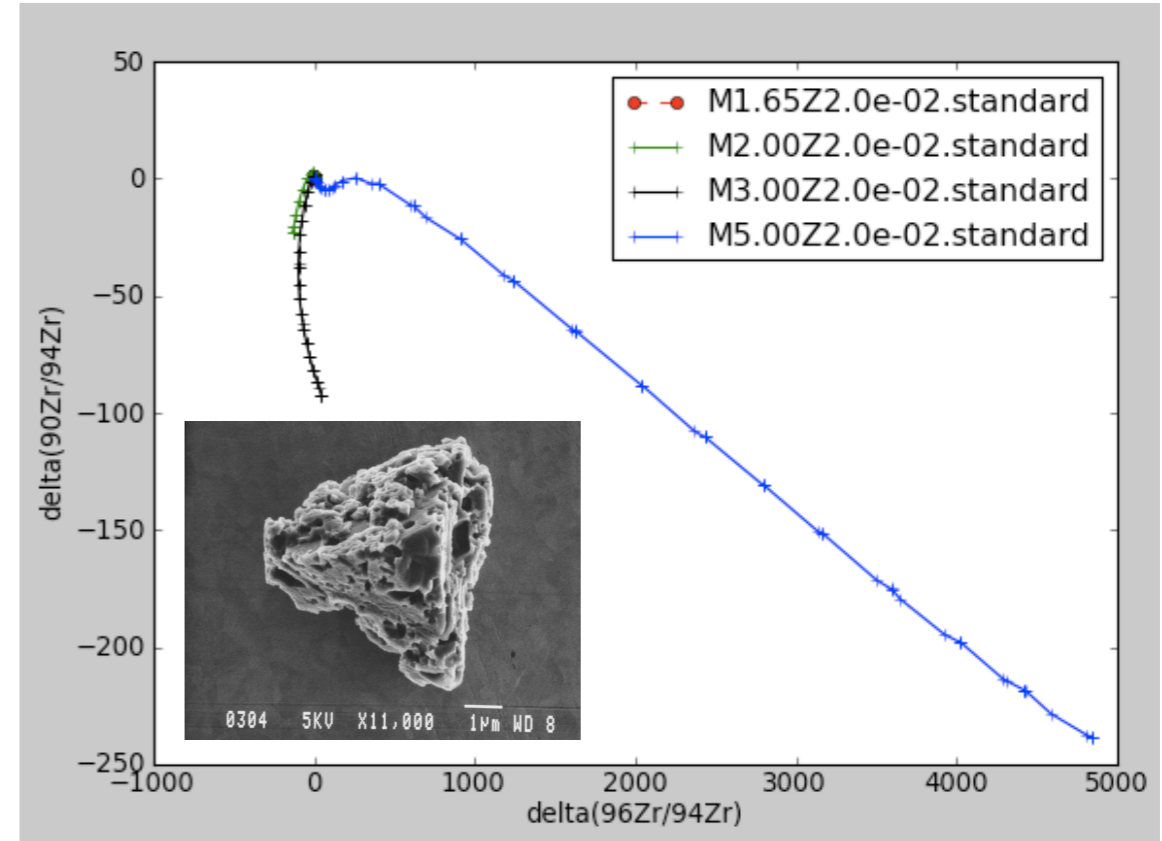


Figure 7 Detail of the chart of isotopes from zirconium to molybdenum. Unstable isotopes are represented in yellow. The *thicker red line* shows the main path of the *s* process; the *thinner red line* shows generally less important side branches. The additional numbers in the boxes give the half-life of unstable isotopes and the isotopic abundance fraction for the stable isotopes.



Lugaro et al 2003

Overview low- and intermediate mass stars I

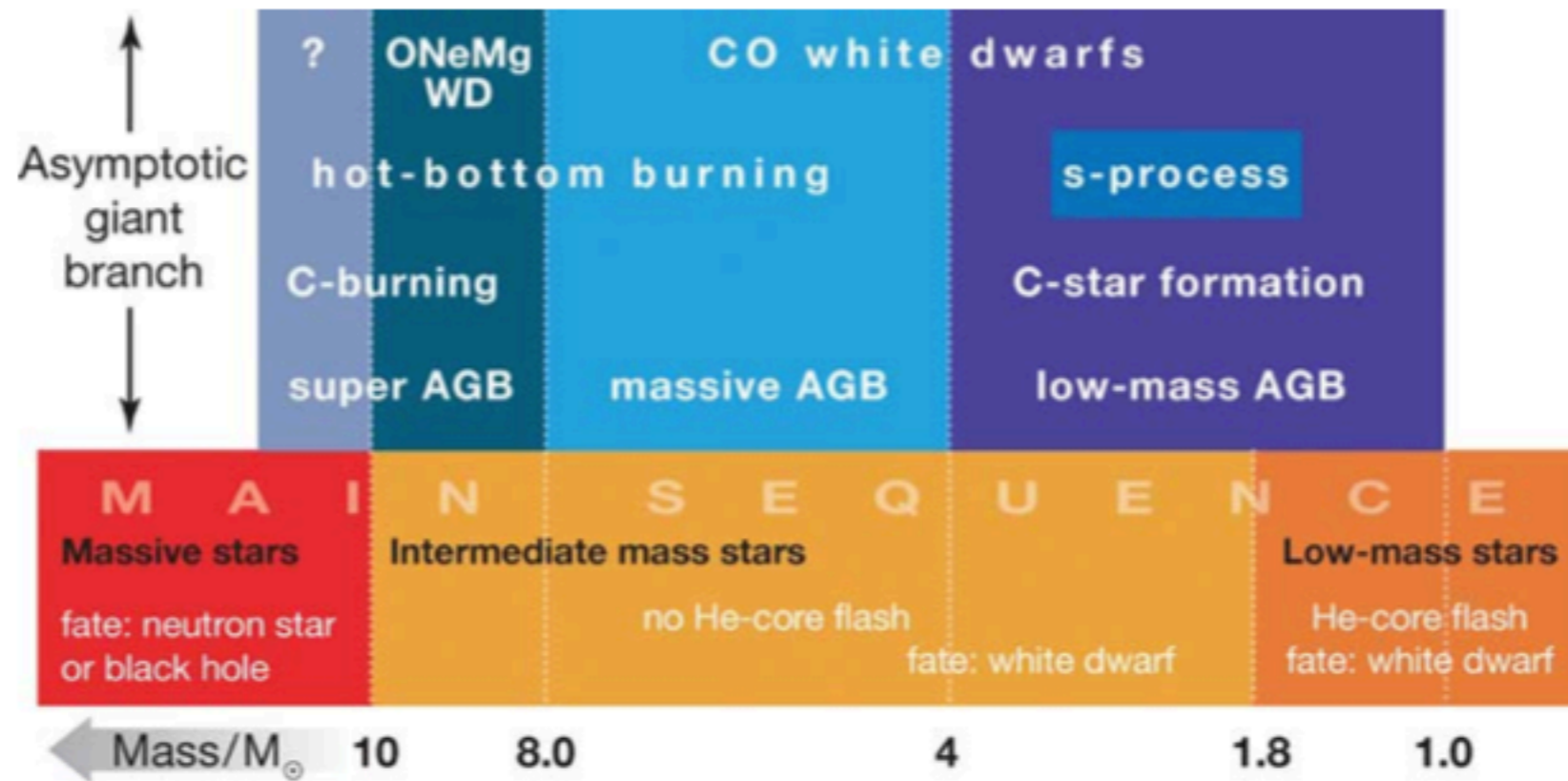


Figure 2 Classification of stars by mass on the main sequence (*lower part*) and on the AGB (*upper part*). The *lower part* shows mass designation according to initial mass. The *upper part* indicates the mass classification appropriate for AGB stars. Approximate limiting masses between different regimes are given at the bottom. These estimates are dependent on physics assumptions and input of models, as well as on metallicity. The different regimes have been labeled with some characterizing properties. The evolutionary fate of super-AGB stars is still uncertain (Section 5).

Herwig 2005, ARAA

Overview low- and intermediate mass stars II

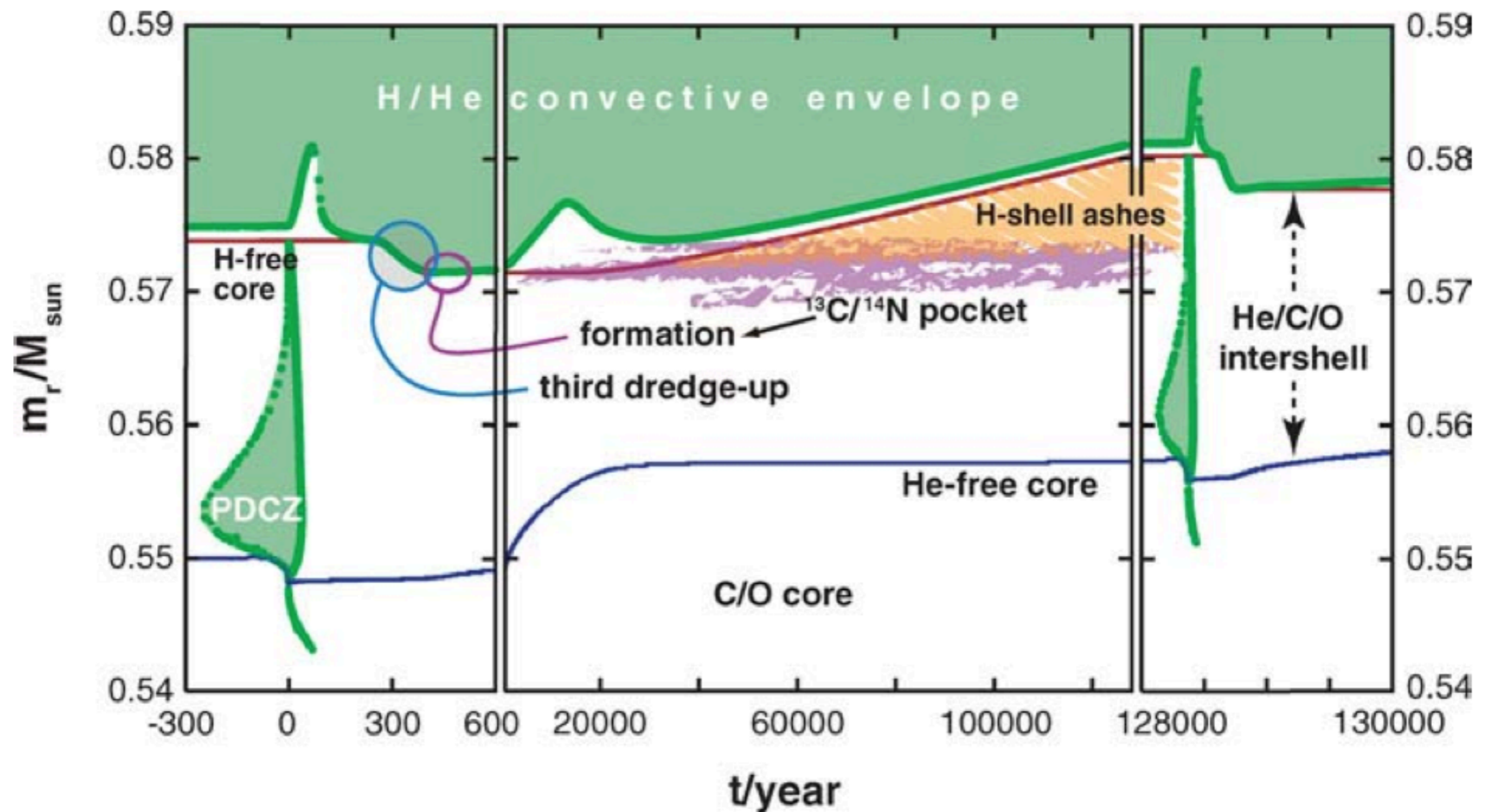
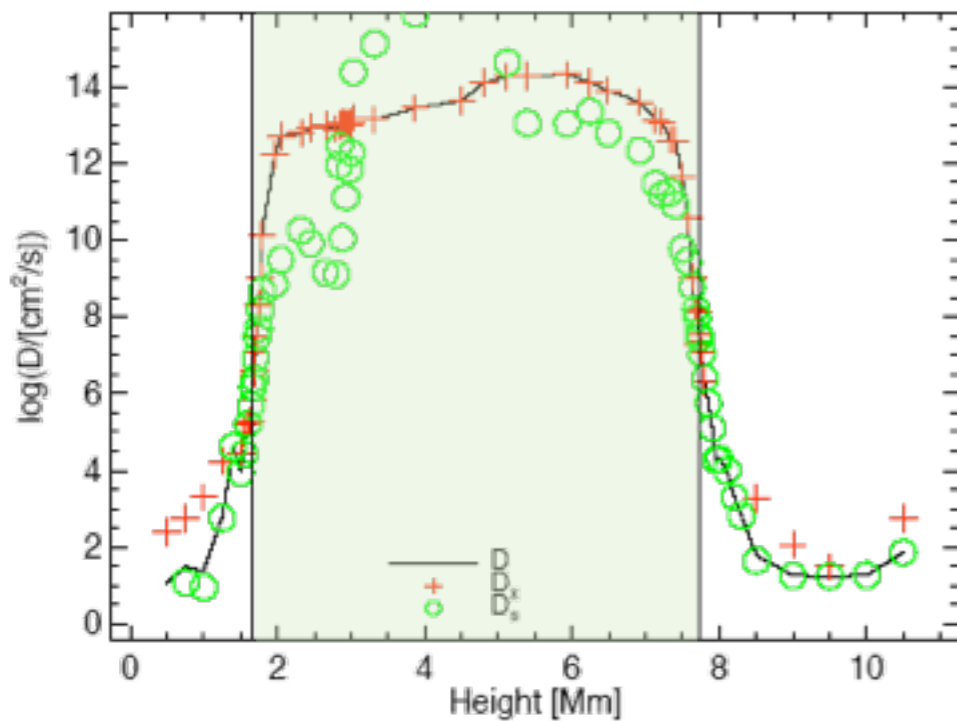
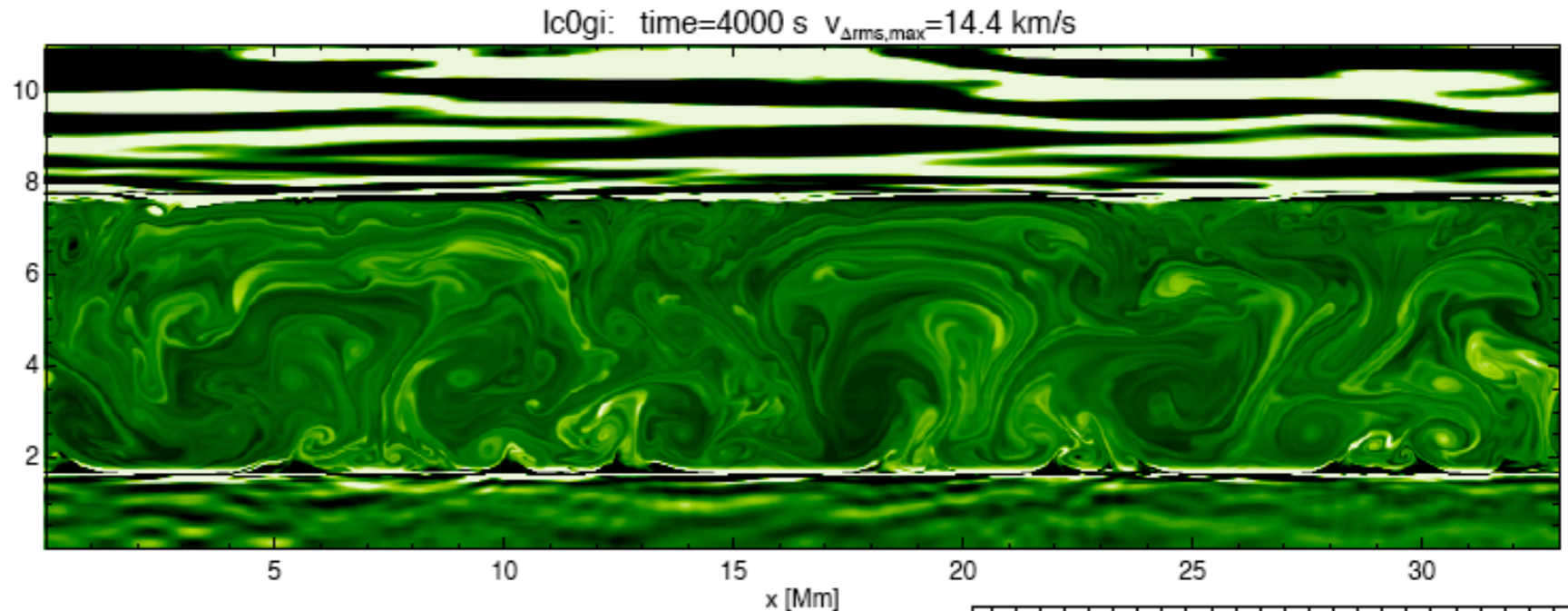


Figure 3 Thermal pulse 14, the subsequent interpulse phase and thermal pulse 15 of $2 M_{\odot}$, $Z = 0.01$ sequence ET2 of Herwig & Austin (2004). The timescale is different in each panel. The *red solid line* indicates the mass coordinate of the H-free core. The *dotted green line* shows the boundaries of convection; each *dot* corresponds to one model in time. Convection zones are *light green*. The shown section of the evolution comprises 12,000 time steps. The colors indicating convection zones, layers with H-shell ashes and the region of the ^{13}C pocket match those in Figure 5.

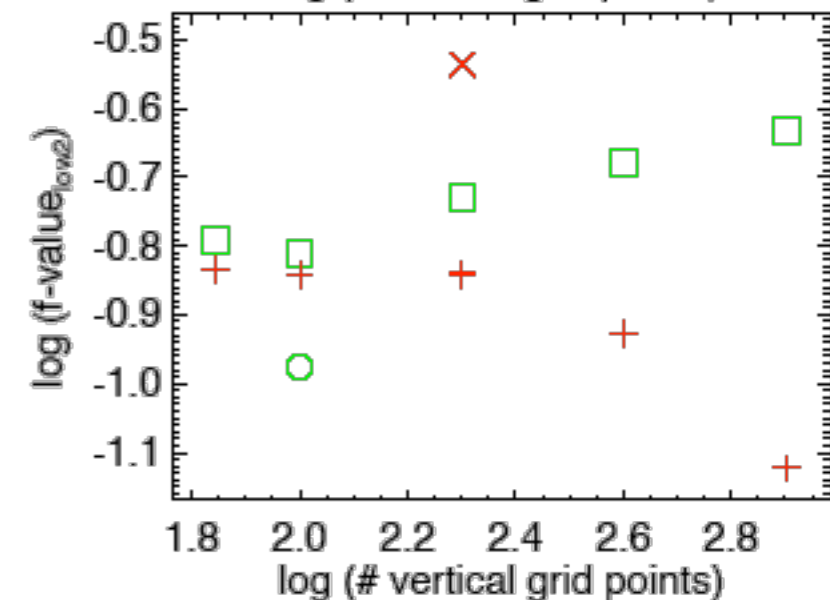
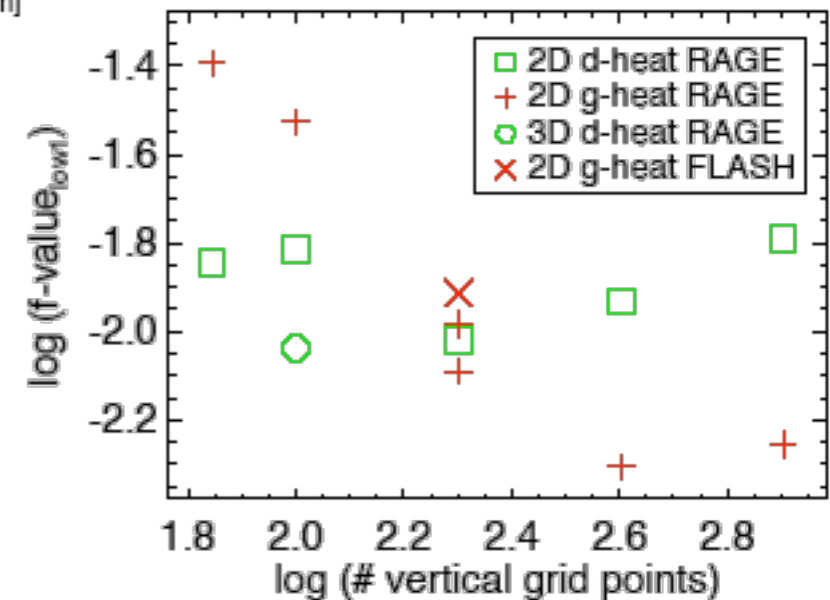
Multi-dimensional stars

He-shell flash convection

2D and 3D plane-parallel box-in-a-star (Herwig et al 2006)



2D entropy fluctuations (2400x800), realistic heating rate
Courant time scale at this resolution:
 $\sim 3 \cdot 10^{-3}$ sec \rightarrow 1.6M cycles



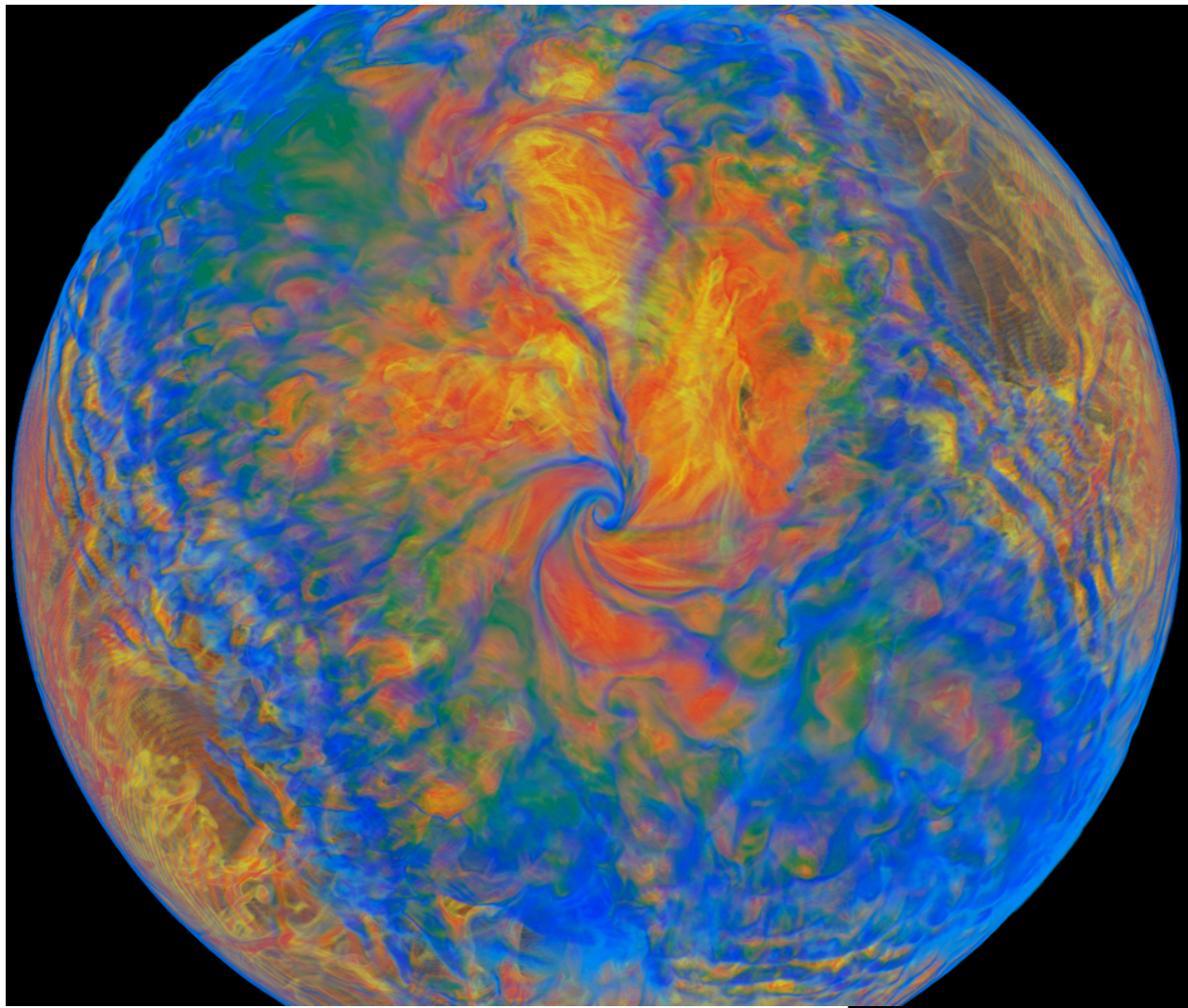
quantify "overshooting" - develop models for 1D stellar evolution

Herwig et al, 2008
Freytag & Herwig, in prep

$$f_{\text{top}} \sim 0.10$$

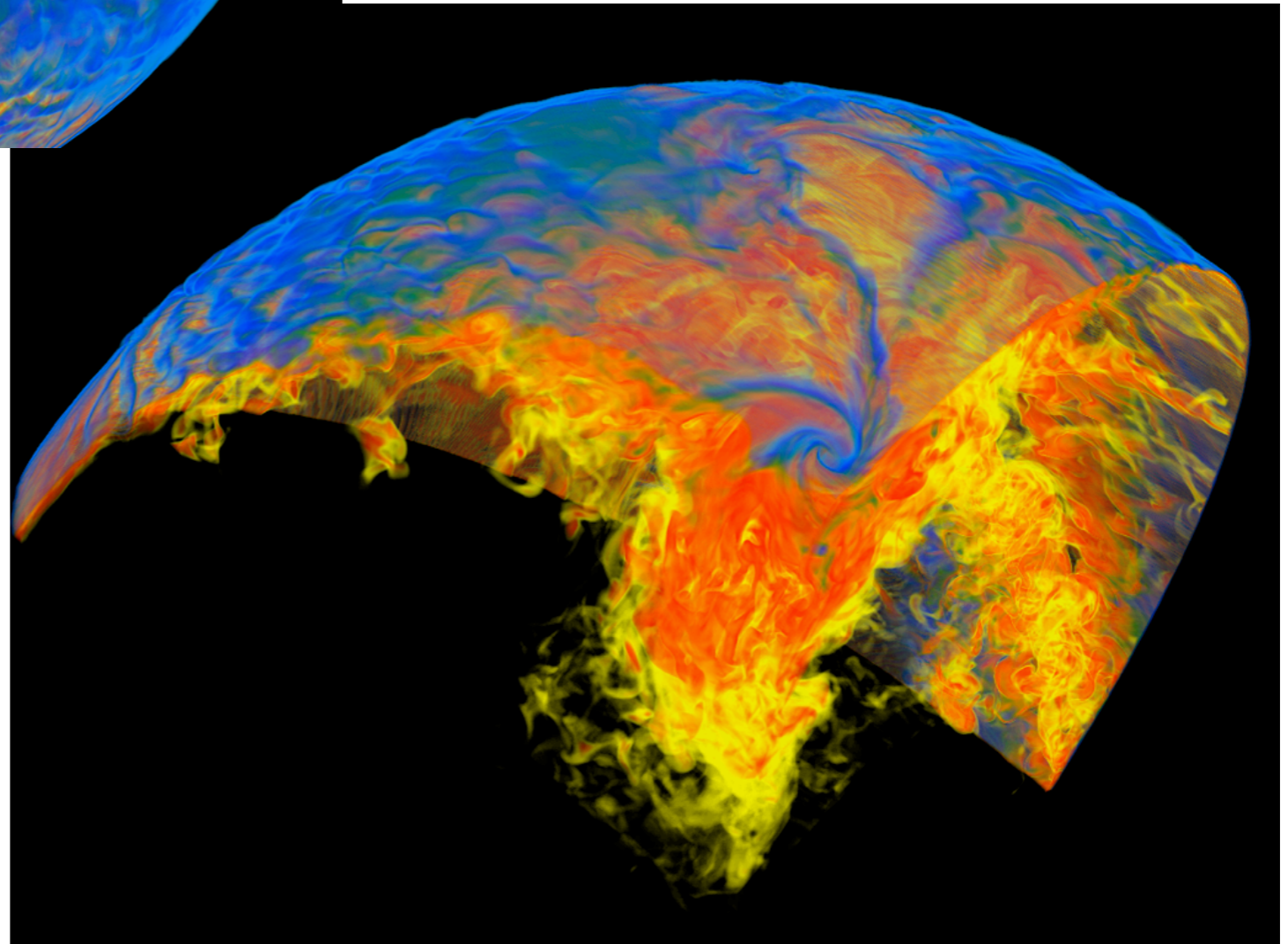
$$f_{\text{bot},1} \sim 0.01$$

$$f_{\text{bot},2} \sim 0.14$$



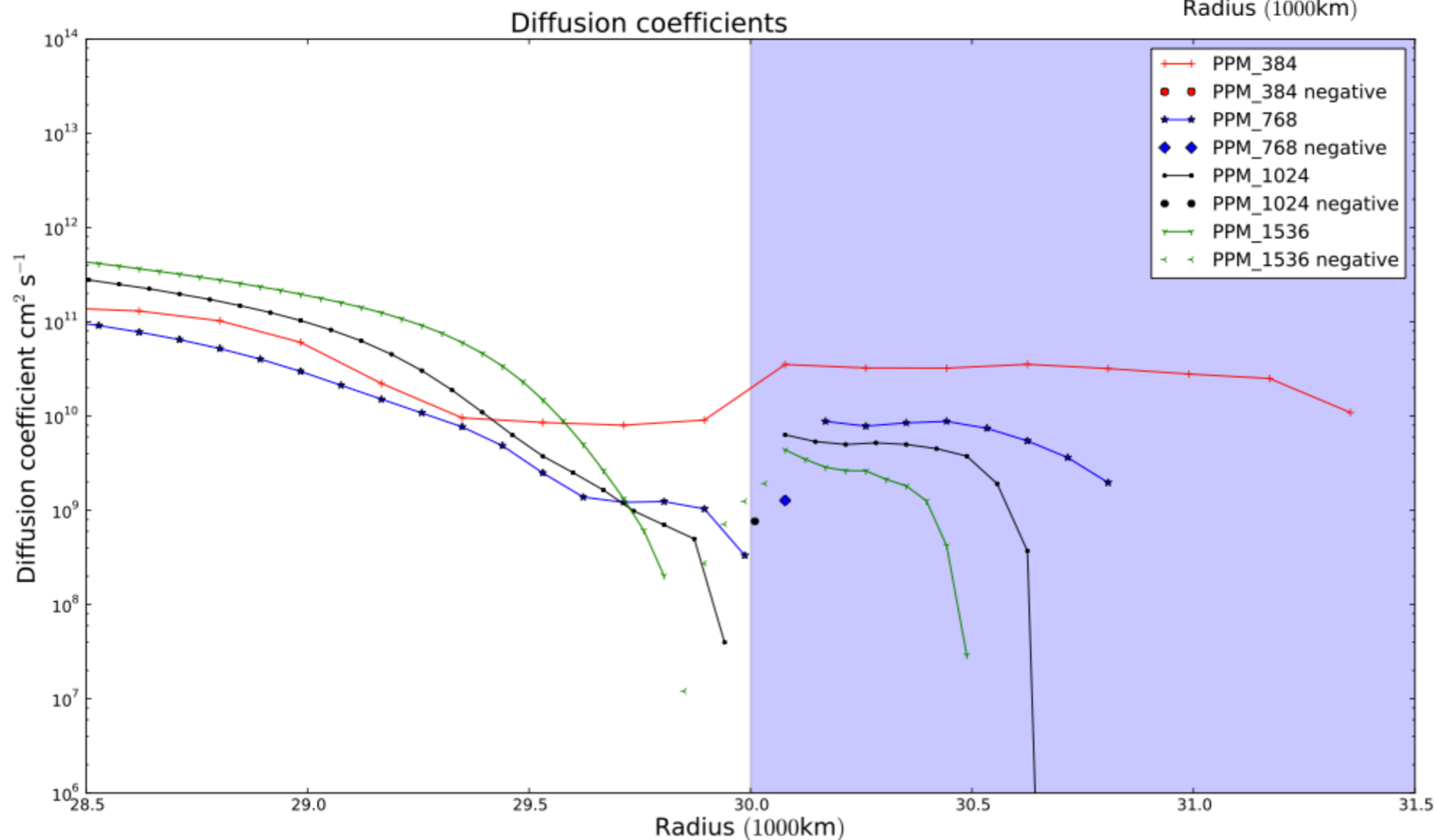
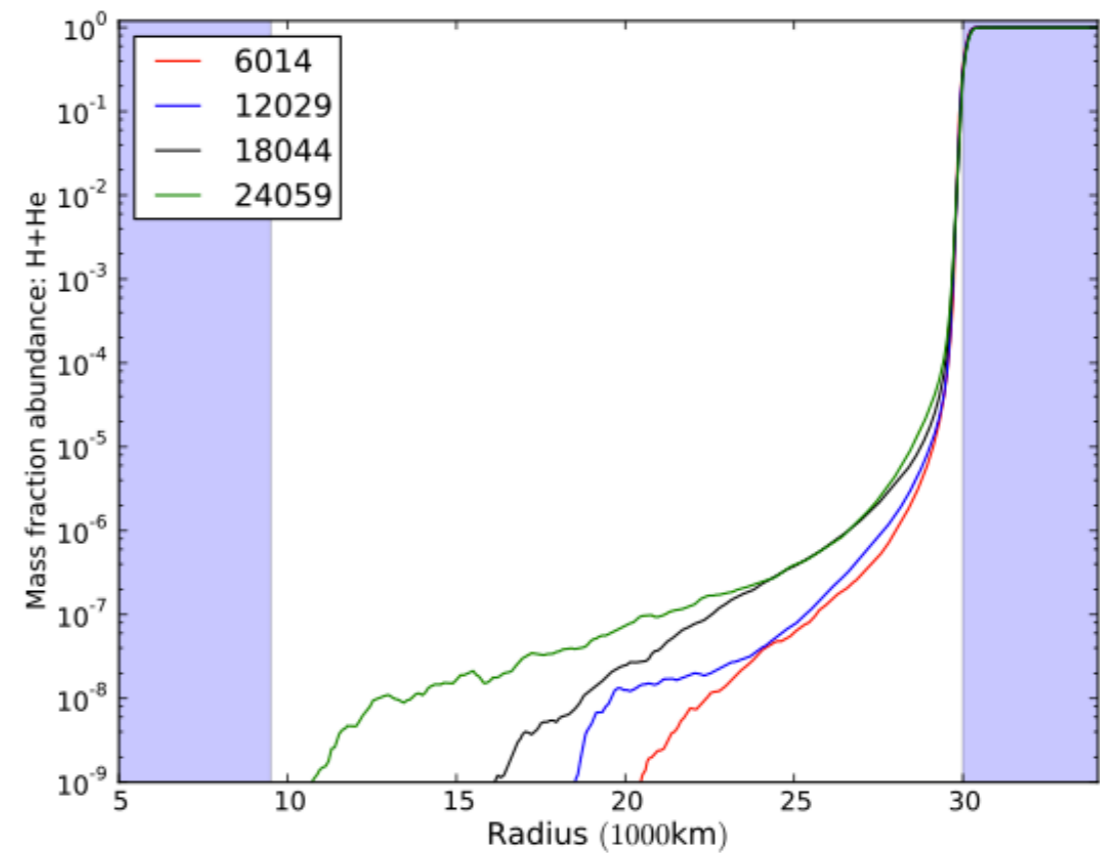
Entrainment He-shell flash convection

4 π 3D simulations:
concentration of fluid
“above” (with Woodward,
LCSE Minnesota)

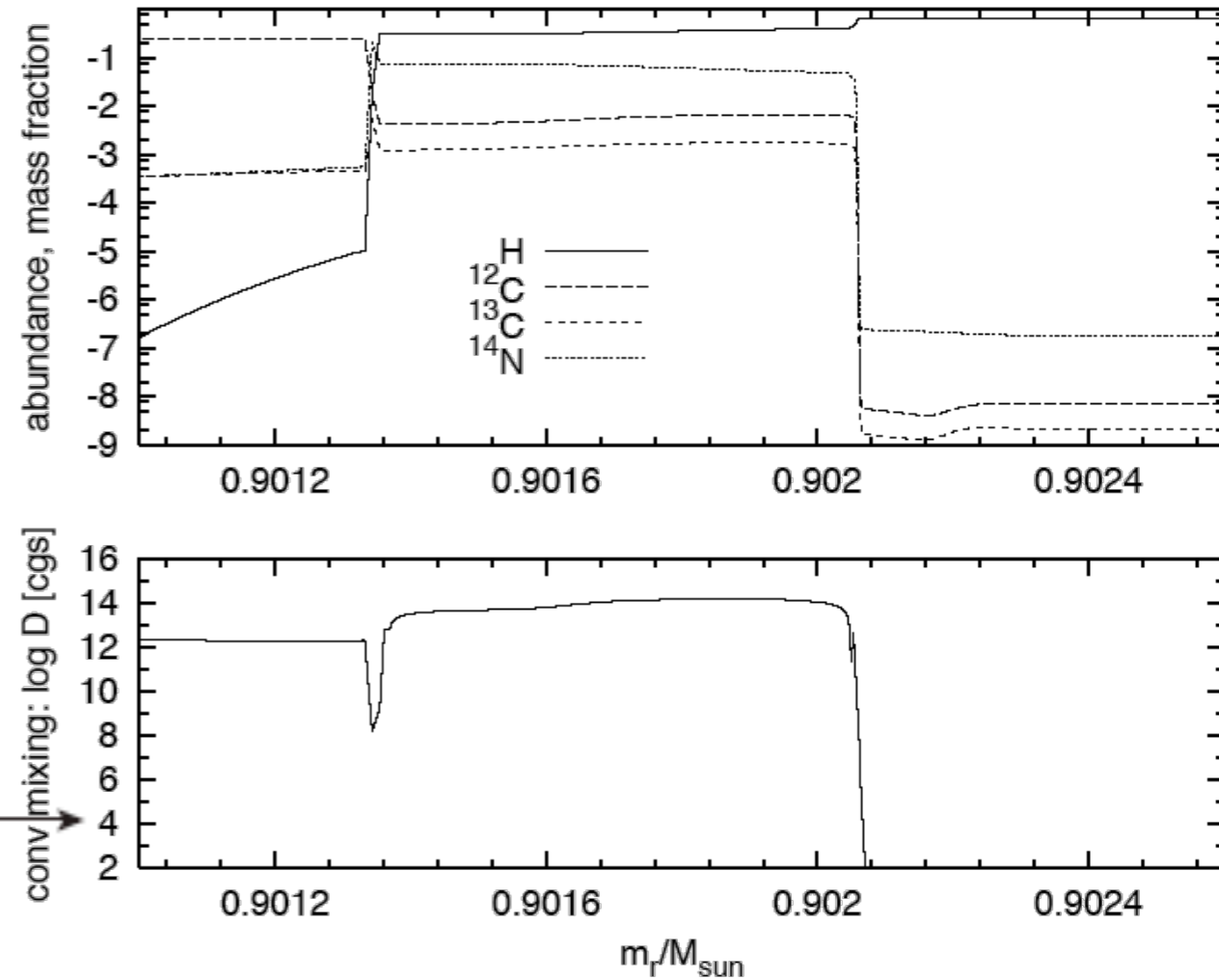
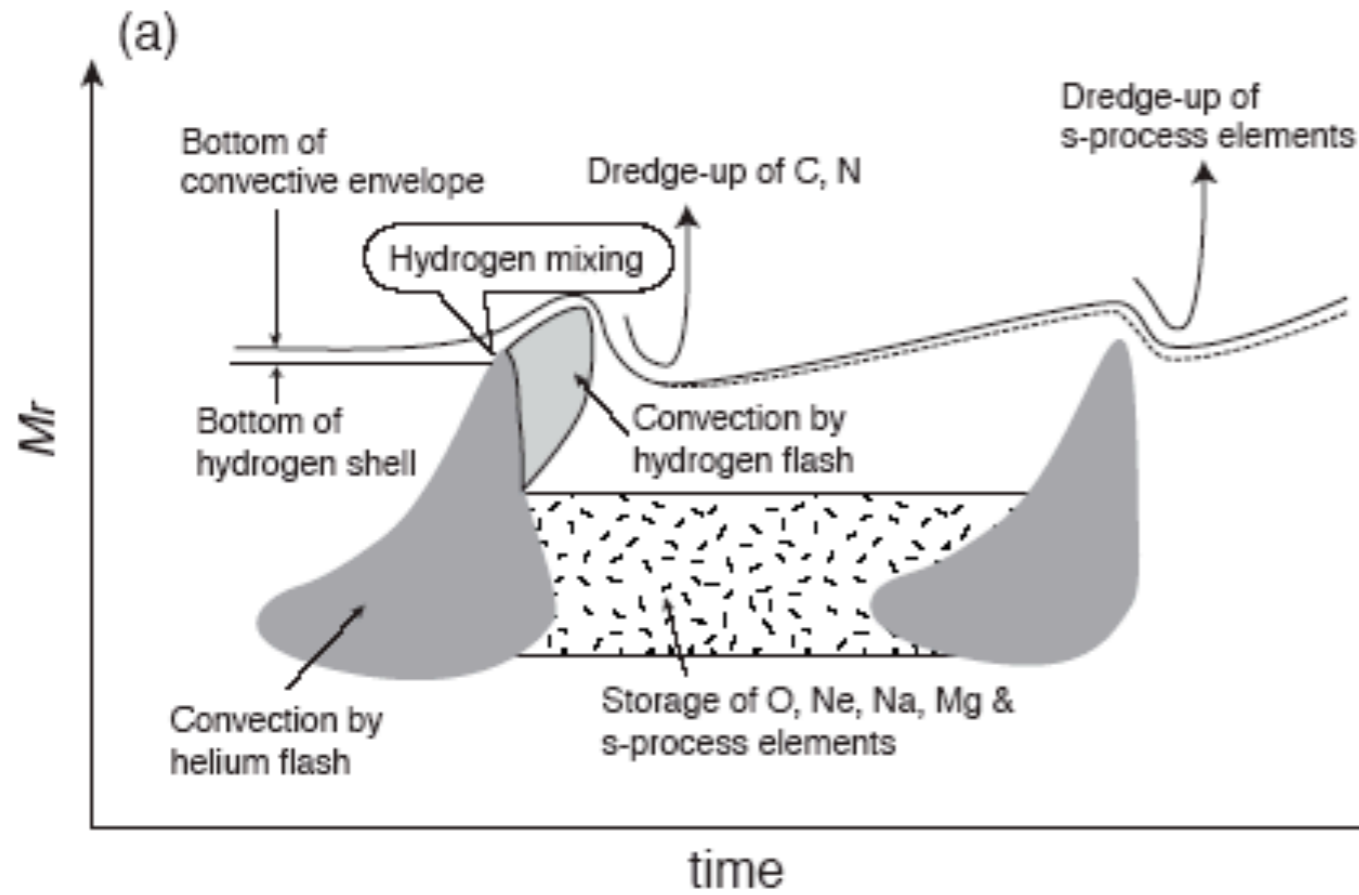


Building sub-grid models for 1D stellar evolution

diffusion coefficient analysis
(with Michael Bennett@Keele)

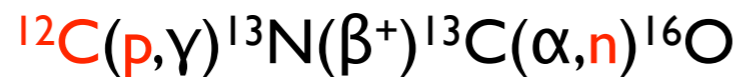


The H-ingestion (core/shell) flash in low-metallicity RGB/AGB stars



For $[Fe/H] < -2.5$ (Suda et al. 2004)

Iwamoto et al (2004): the site for s-process in EMP AGB stars



$5M_{\text{sun}}, Z=0.0, 10\text{th TP, Herwig 2002}$

see also more recent work by:

Campbell et al

Cristallo et al

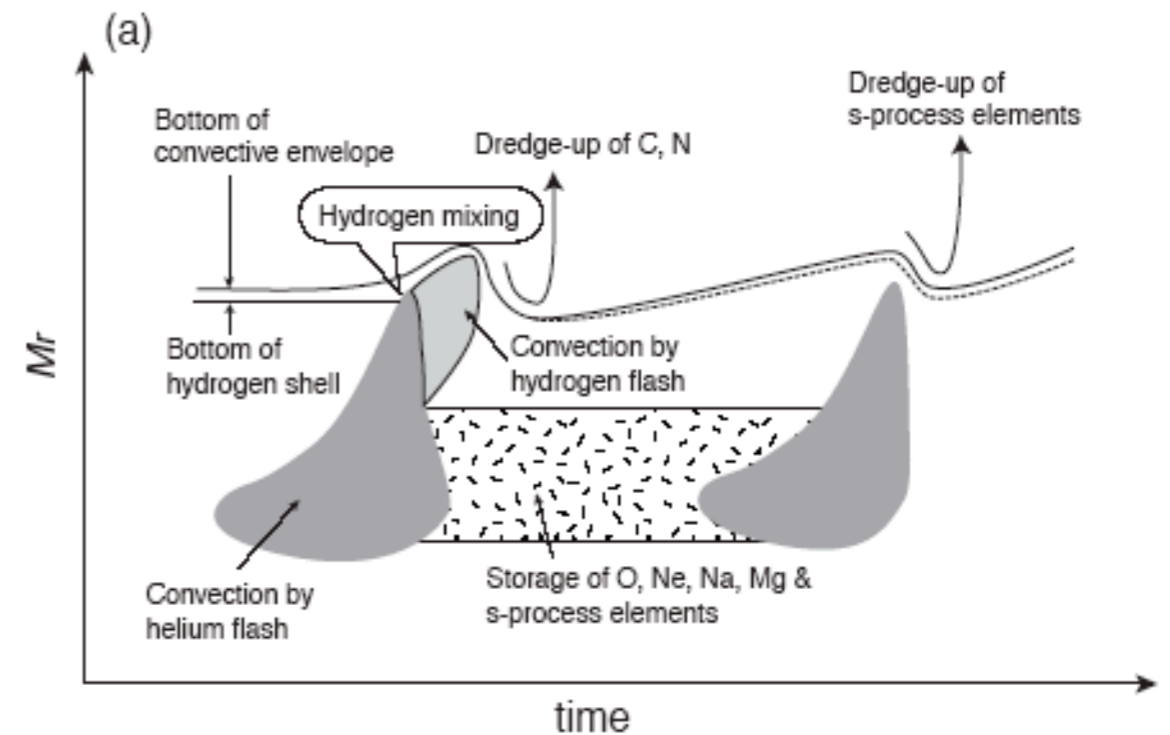
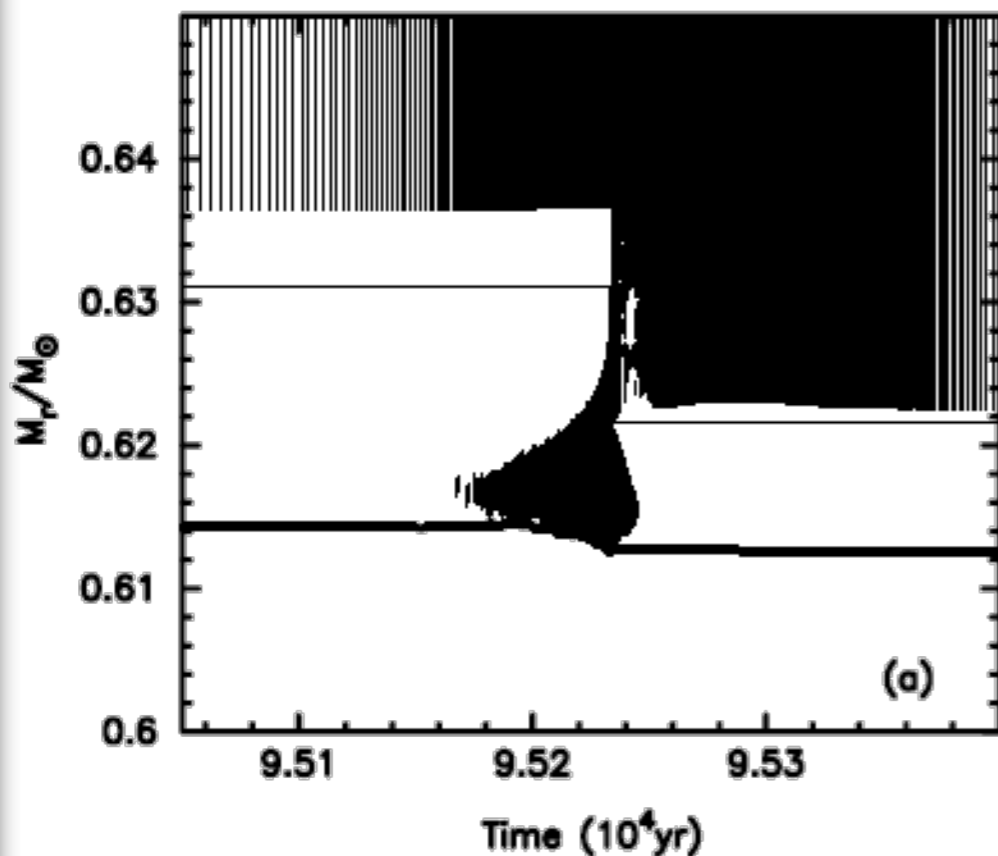
Lau et al and others

More examples

Numerous instances of convective-reactive phases in the literature, in the context of Pop III:

Fujimoto et al. (1990), Hollowell et al. (1990), Iwamoto et al (2004), Fujimoto et al (2000), Herwig (2003), Chieffi et al (2001), Weiss et al. (2004), Schlattl et al (2001), Picardie et al (2004), Suda et al (2004) ...

2Msun, Z=0

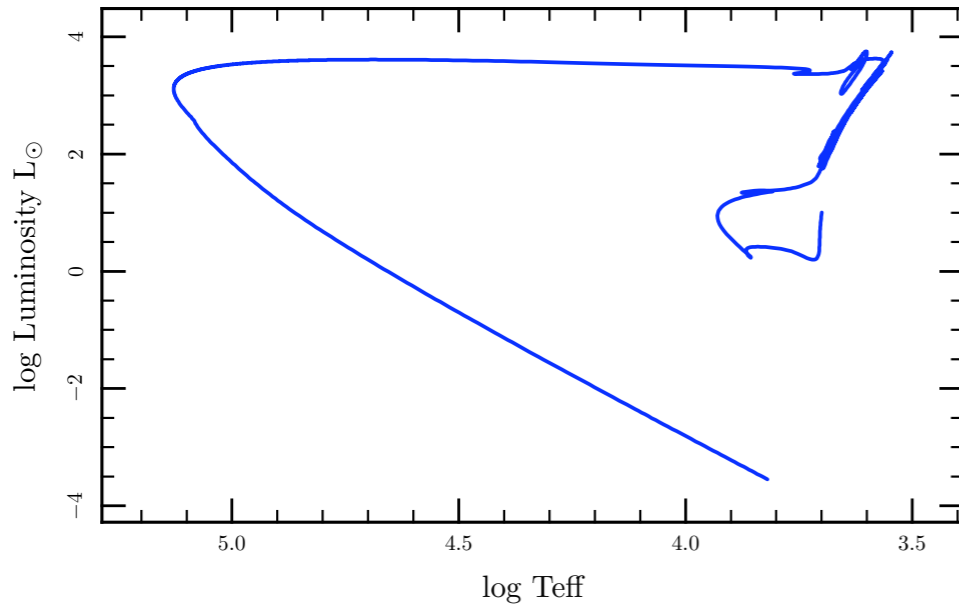
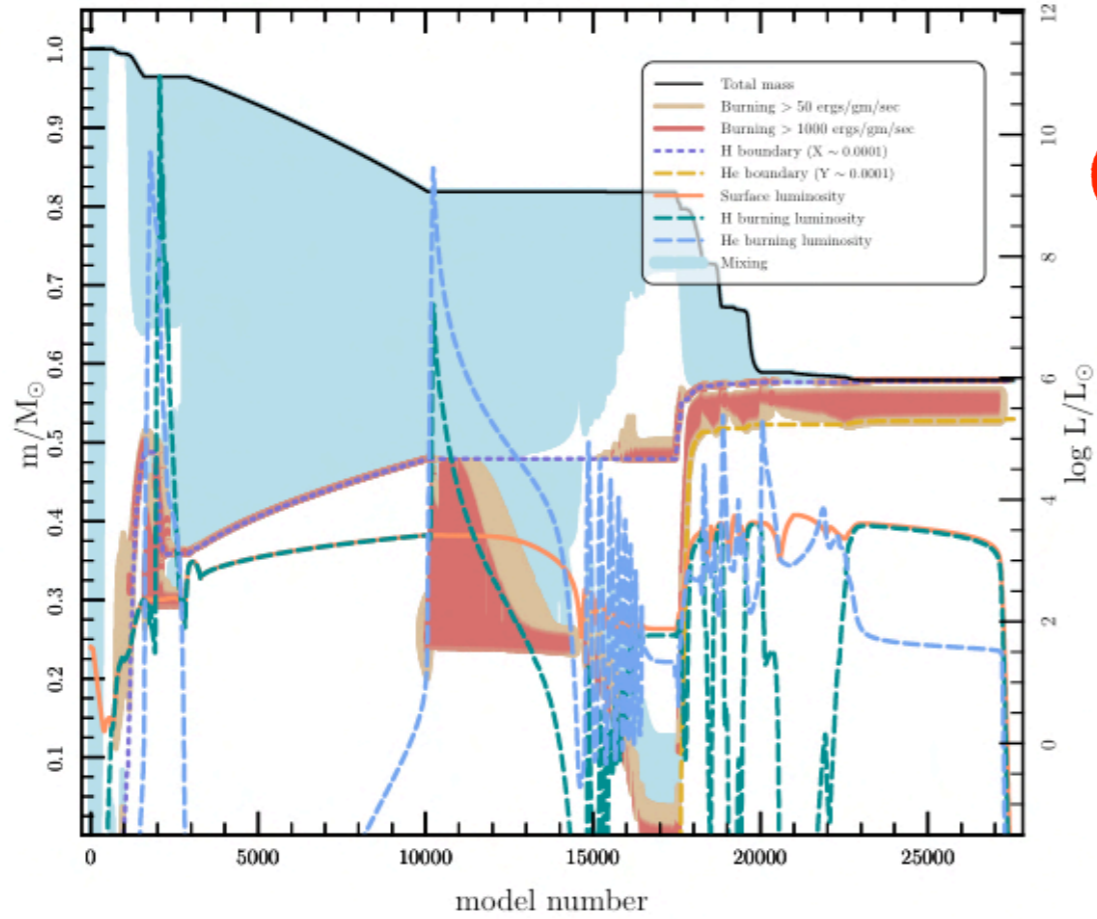


... also in massive Pop III and II.5 and X-ray bursts.

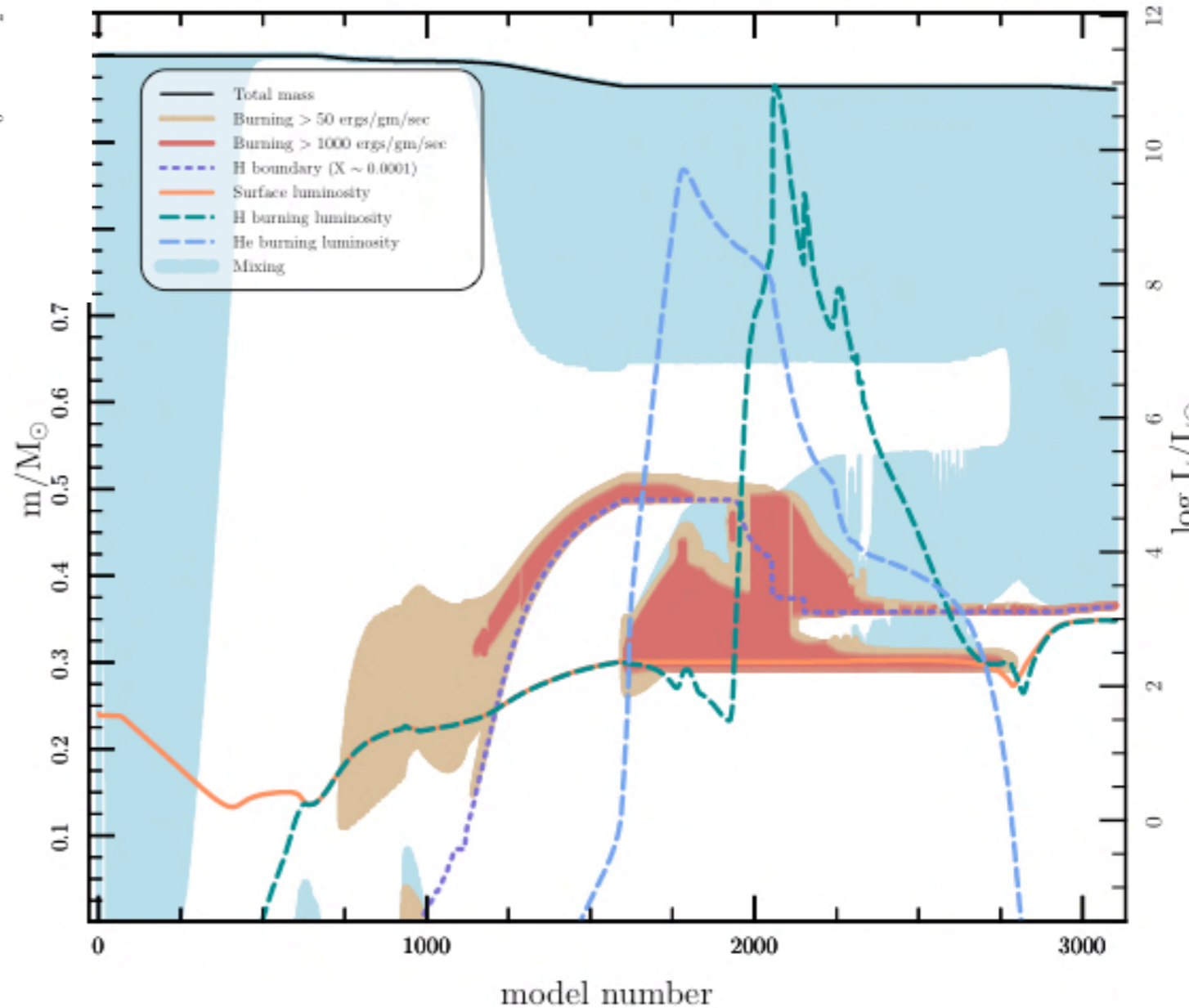
Iwamoto et al. 2004

Convective-reactive event in $1M_{\odot}$ Pop III stellar models (with MESA code, Bill Paxton)

Internal Structure: $M=0.579$, initial $Z=0$



Internal Structure: $M=0.961$, initial $Z=0$





Other examples at near-solar metal content:

- X-ray bursts (Woosely et al 2004, Piro & Bildsten 2007)
- accreting white dwarfs, SNIa progenitors (Cassisi et al 1998)
- post-RGB late He-flashers (Brown et al 2001, Miller Bertolami et al 2008)
- post-AGB He-flashers (Schönberner 1979; Iben 1983, 1995; Herwig et al 1999, 2001; Miller-Bertolami et al 2006)

H-combustion in stellar evolution

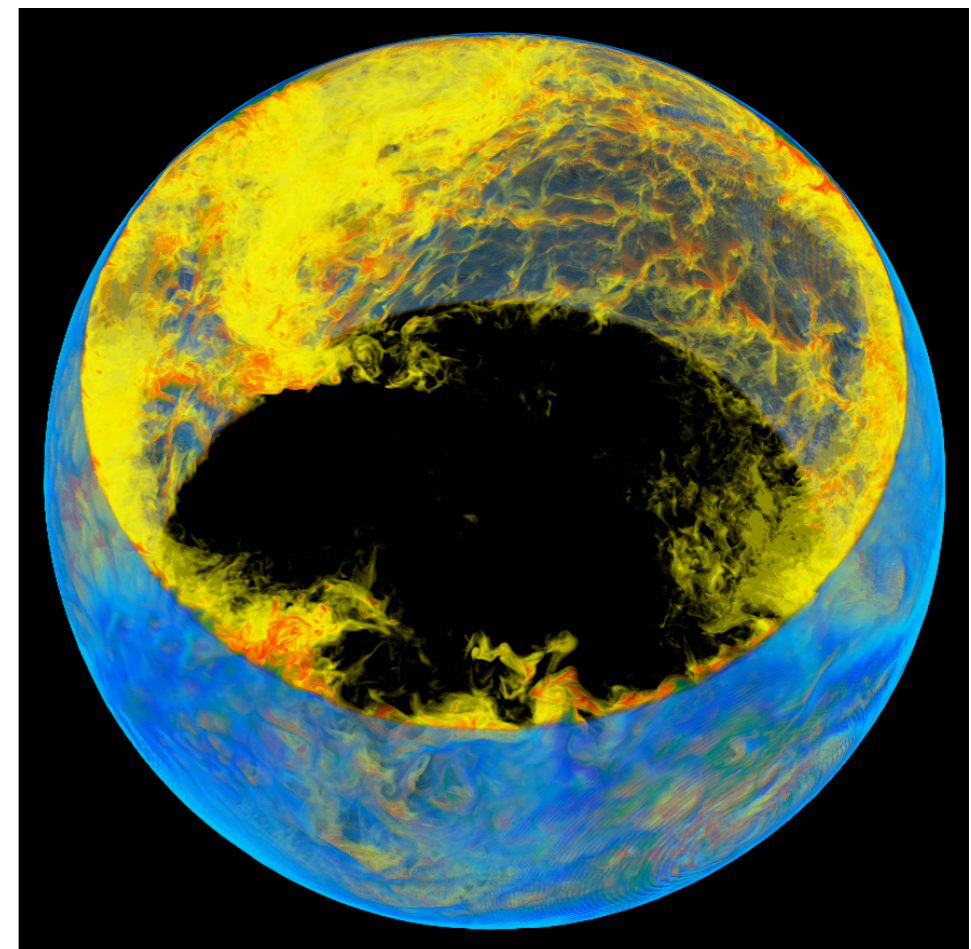
convective mixing of H into ^{12}C -rich He-convection zone
 $T \sim 150\text{-}300\text{MK}$, $\tau_{\text{mix}} \sim 1000$

The ratio of the mixing time scale and the reaction time scale is called the Damköhler number:

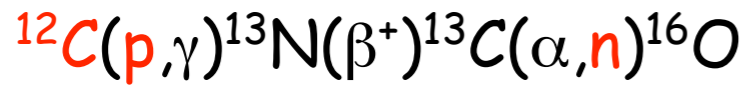
$$D_{\alpha} = \frac{\tau_{\text{mix}}}{\tau_{\text{react}}} .$$

Dimotakis, P. E. 2005, Annu. Rev. Fluid Mech., 37, 329

- $D_{\alpha} \ll 1$: fully mixed burning, MLT appropriate
- $D_{\alpha} \sim 1$: combustion regime, MLT and 1D spherical symmetry assumption inappropriate because:
 - ★ MLT describes convection only in a time and spatially averaged sense
 - ★ in combustion fuels are not completely mixed
 - ★ fluid elements have a range of velocity - broadens the burning front
 - ★ localized energy feedback from nuclear burn feeds back into hydro



H-combustion provides naturally a neutron source under "non-standard" conditions



	O 12	O 13 8,58 ms β^+ 16,7... βp 1,44; 6,44... γ (4439*, 3500...)	O 14 70,59 s β^+ 1,8; 4,1... γ 2313...	O 15 2,03 m β^+ 1,7 no γ	O 16 99,762 σ 0,00019	O 17 0,038 $\sigma_{n,\alpha}$ 0,24	O 18 0,200 σ 0,00016	O 19 27,1 s β^- 3,3; 4,7... γ 197; 1357...	O 20 13,5 s β^- 2,8... γ 1057...	
	N 11	N 12 11,0 ms β^+ 16,4... γ 4439... $\beta\alpha$ 0,2...	N 13 9,96 m β^+ 1,2 no γ	N 14 99,634 σ 0,080 $\sigma_{n,p}$ 1,8	N 15 0,366 σ 0,00004	N 16 5,3 μ s 7,13 s β^- 4,3; 10,4... γ 8129; 7115... βn 1,76...	N 17 4,17 s β^- 3,2; 8,7... βn 1,17; 0,38... γ 871; 2184; $\beta\alpha$ 1,25; 1,41	N 18 0,63 s β^- 9,4; 11,9... γ 1880; 822; 1652; 2473... $\beta\alpha$ 1,68; 1,41... βn 1,35; 2,46...	N 19 329 ms β^- βn γ 96; 3138; 709	
	C 9 126,5 ms β^+ 15,5... βp 8,24; 10,92... $\beta\alpha$	C 10 19,3 s β^+ 1,9... γ 718; 1022	C 11 20,38 m β^+ 1,0 no γ	C 12 98,90 σ 0,0035	C 13 1,10 σ 0,0014	C 14 5730 a β^- 0,2 no γ	C 15 2,45 s β^- 4,5; 9,8... γ 5298...	C 16 0,747 s β^- 4,7; 7,9... βn 0,79; 1,72	C 17 193 ms β^- βn 1,62... γ 1375; 1849; 1906...	C 18 92 ms β^- γ 2614; 880; 2499... βn 0,88; 1,55...
	B 8 770 ms β^+ 14,1... $\beta 2\alpha$ ~ 1,6; 8,3	B 9	B 10 19,9 σ 0,5 $\sigma_{n,\alpha}$ 3840	B 11 80,1 σ 0,005	B 12 20,20 ms β^- 13,4... γ 4439... $\beta\alpha$ 0,2...	B 13 17,33 ms β^- 13,4... γ 3684 βn 3,8; 2,4...	B 14 13,8 ms β^- 14,0... γ 6090; 6730 βn	B 15 10,4 ms β^- βn 1,77; 3,20...		B 17 5,1 ms β^- βn ; $\beta 2n$; $\beta 3n$; $\beta 4n$
	Be 7 53,29 d ϵ γ 478 $\sigma_{n,p}$ 39000	Be 8	Be 9 100 σ 0,008	Be 10 $1,6 \cdot 10^6$ a β^- 0,6 no γ	Be 11 13,8 s β^- 11,5... γ 2125; 6791... $\beta\alpha$ 0,77...	Be 12 23,6 ms β^- 11,7... βn		Be 14 4,35 ms β^- βn < 0,8; 3,08; 3,52...; $\beta 2n$ γ 3528*; 3680*		12
	Li 6 7,5 σ 0,039 $\sigma_{n,\alpha}$ 940	Li 7 92,5 σ 0,045	Li 8 840,3 ms β^- 12,5 $\beta 2\alpha$ ~ 1,6	Li 9 178,3 ms β^- 13,6... βn 0,7... $\beta\alpha$	Li 10	Li 11 8,5 ms β^- ~ 18,5; 23,4 γ 3368*; 320... βn ; $\beta 2n$; $\beta 3n$; $\beta\alpha$; βt				10

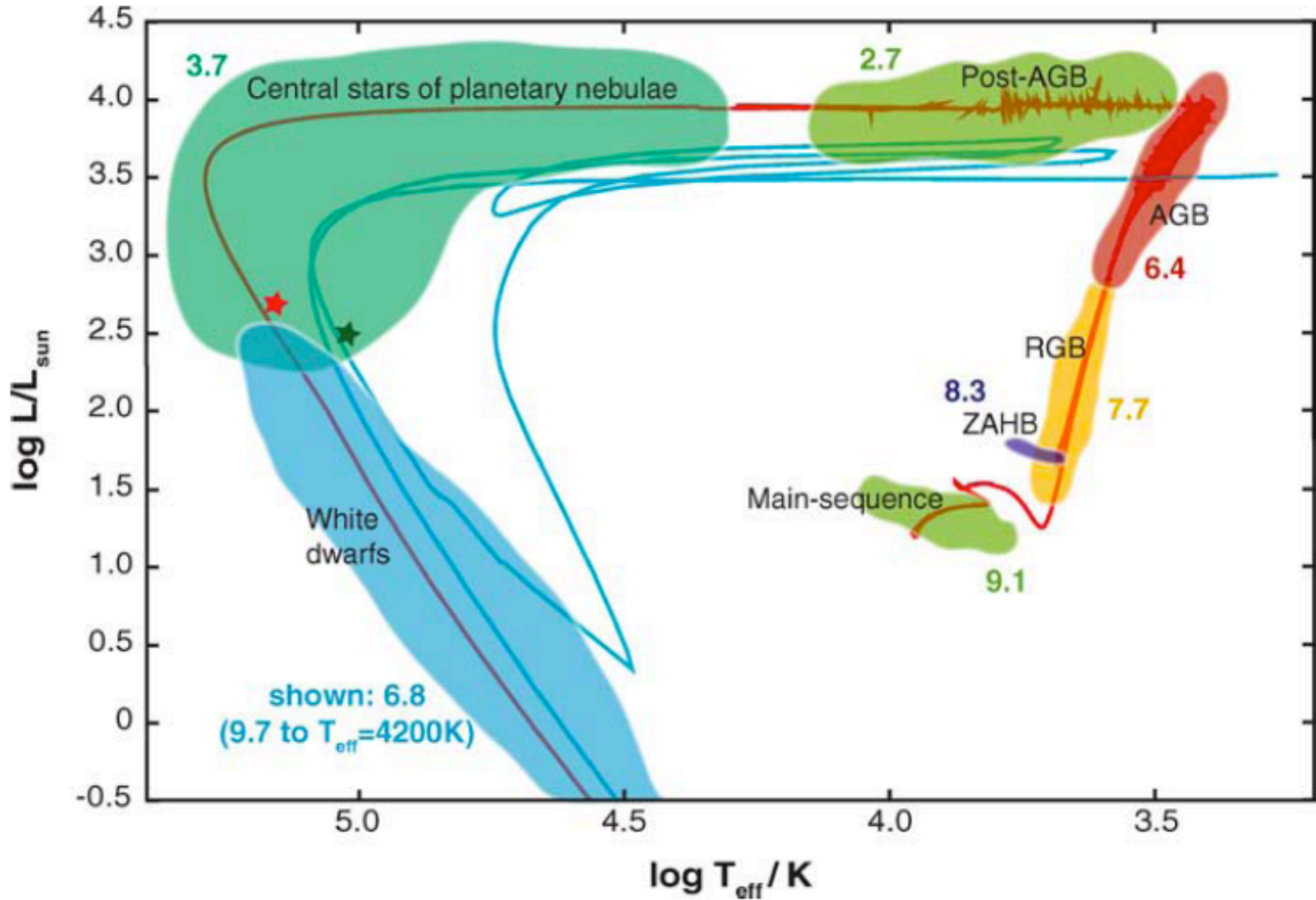


How can we better understand these
H-combustion events?

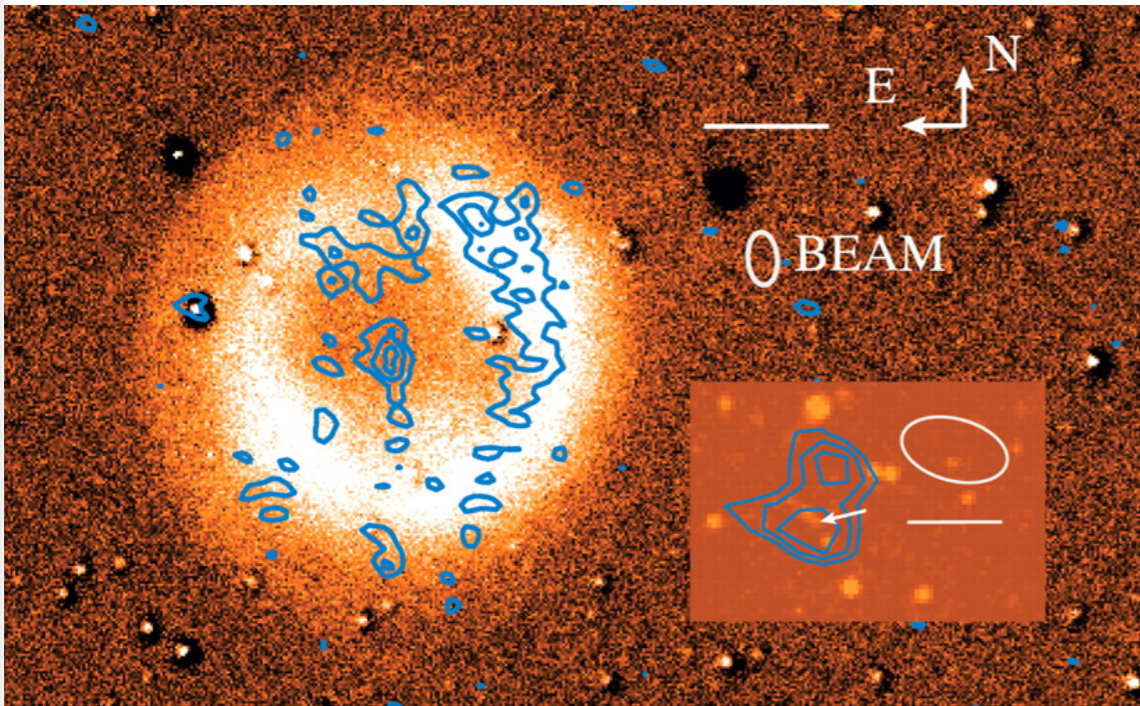
Need cases with many observables that can test
simulations of convective-reactive combustion!

Post-AGB flashers are such validation cases!
Sakurai's object.

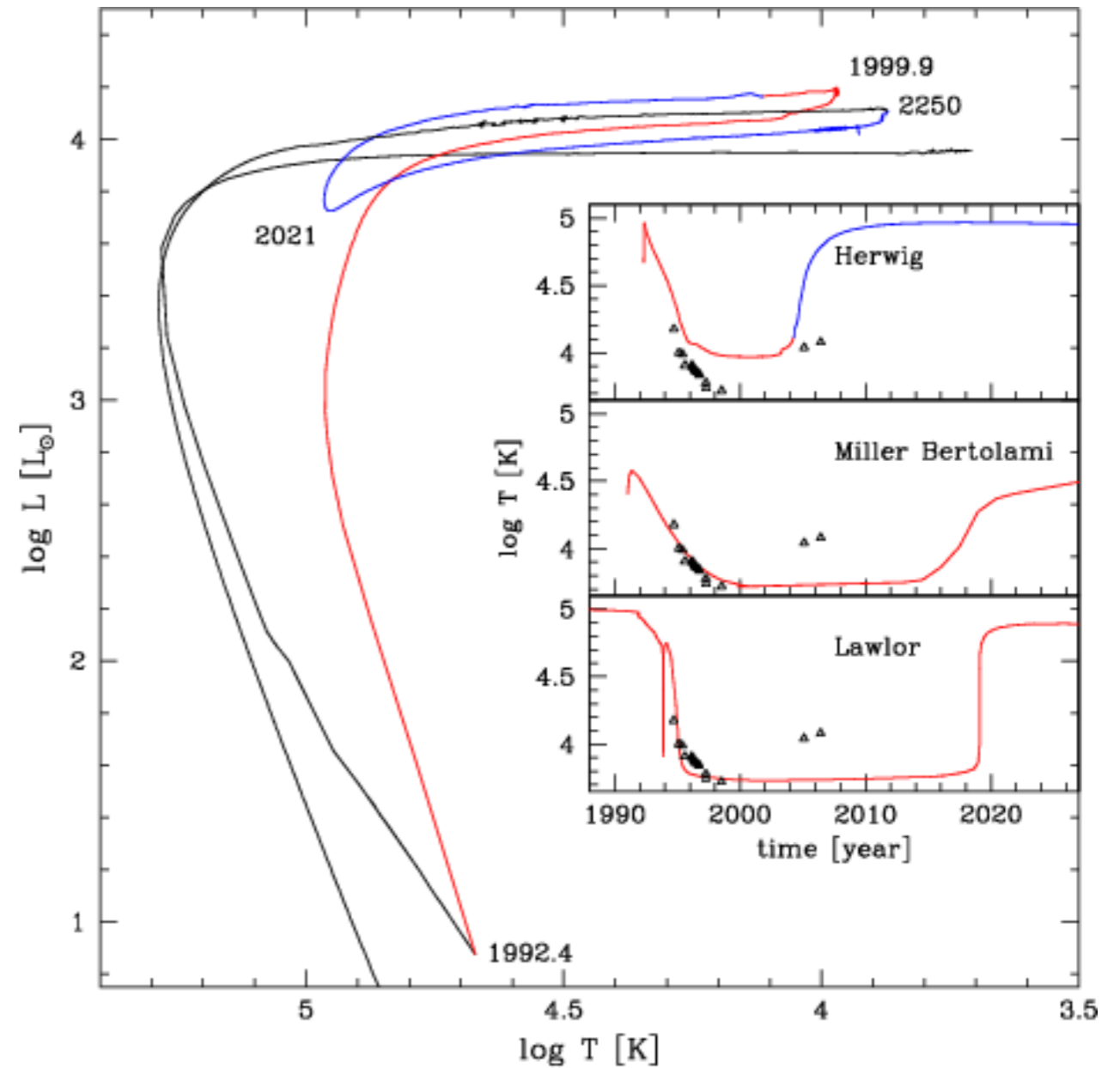
Combustion in the post-AGB flasher



Post-AGB/young white dwarf He-shell flash object
Sakurai's object



Hajduk, Zijlstra, Herwig et al.,
 Science 308, 231, 2005.



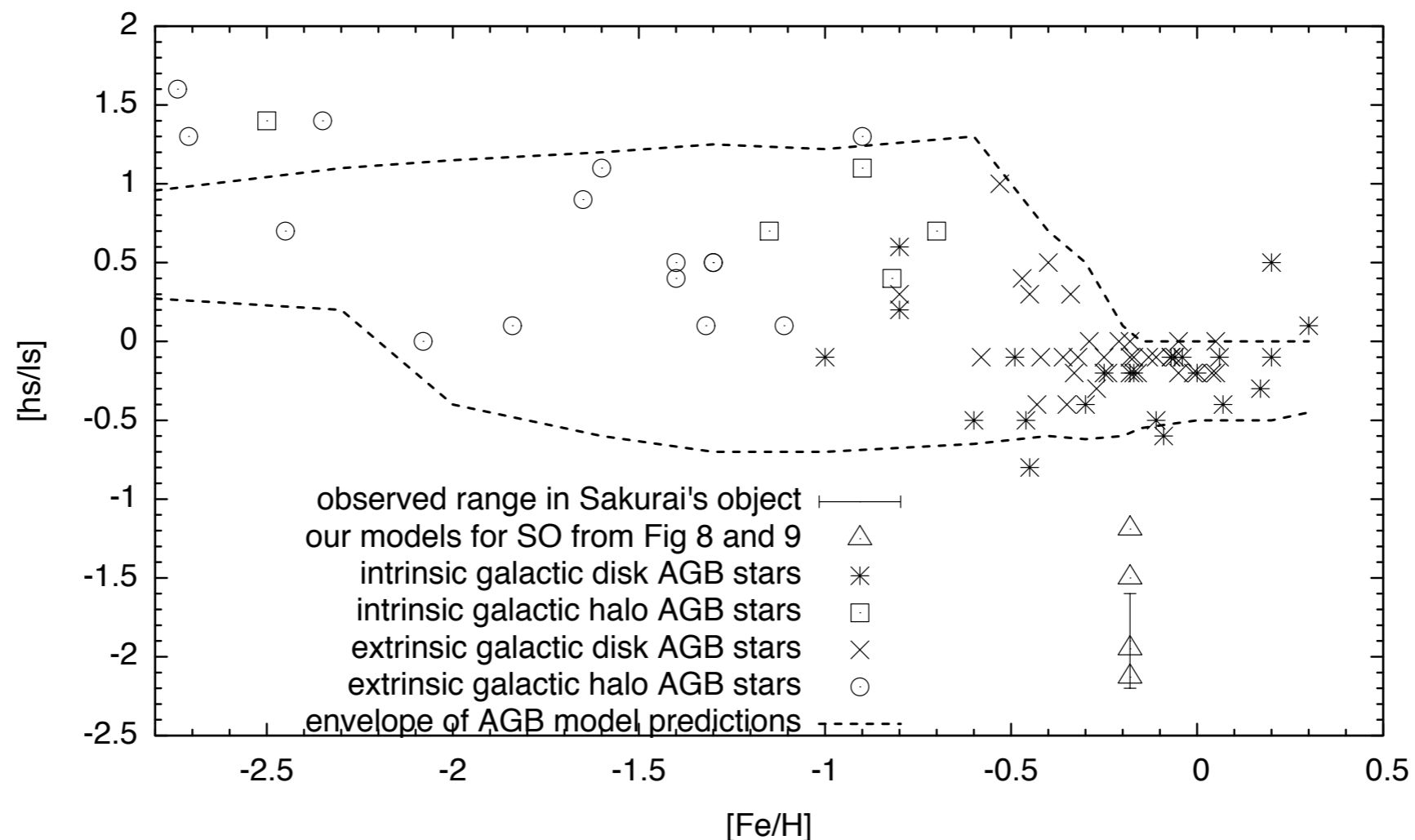
van Hoof et al 2007, 2005/06: radio
 observation with VLA

Highly non-solar, H-deficient abundance distribution of Sakurai's Object in 1996

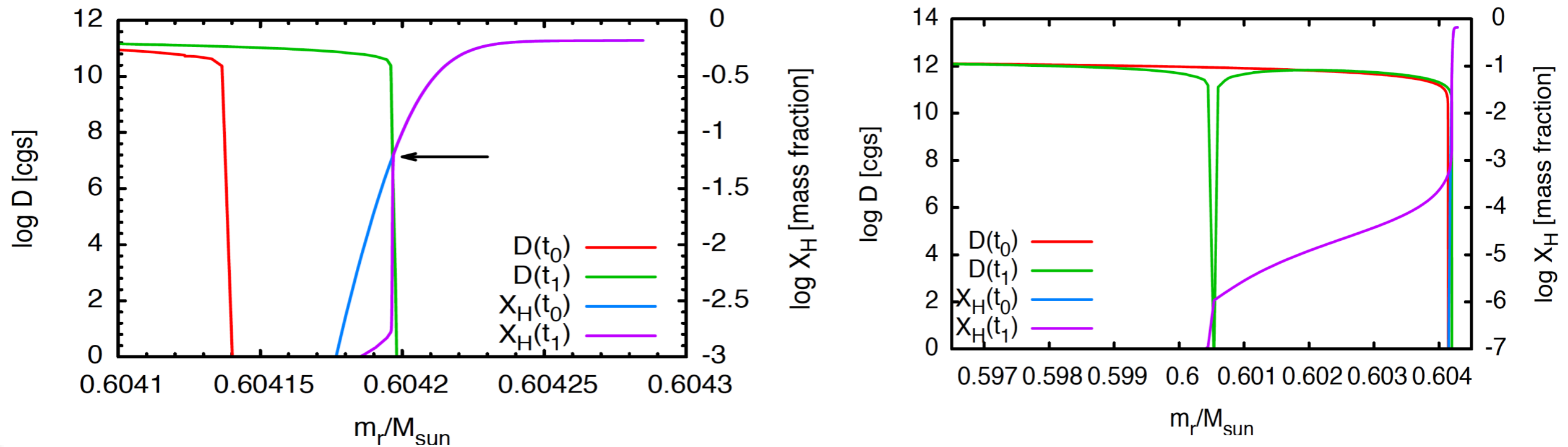
Element	Sun ^a	Sakurai's object in 1996					R CrB majority ^b	V854 Cen ^c
		April 20–25	May 5–9	June 4	July 3	October 7		
H	12.00	10.0	9.7	9.7	9.6	9.0	< 4.1–6.9	9.9
He	10.93	11.4 ^d	11.4 ^d	11.4 ^d	11.4 ^d	11.4 ^d	11.5 ^d	11.4 ^d
Li	3.31	3.6	3.6	3.6	4.0	4.2	< 1.1–3.5	< 2.0
C	8.52	9.7 ^e ± 0.2	9.7 ^e ± 0.2	9.6 ^e ± 0.2	9.7 ^e ± 0.3	9.8 ^e ± 0.3	8.9 ^e	9.6 ^e
N	7.92	9.0 ± 0.3	8.9 ± 0.4	9.0 ± 0.4	9.2 ± 0.3	8.9 ± 0.2	8.6	7.8
O	8.83	9.2 ± 0.2	9.5 ± 0.3	9.3 ± 0.4	9.3 ± 0.1	9.4 ± 0.2	8.2	8.9
Ne	8.08	9.4 ± 0.2	9.4 ± 0.3	9.5 ± 0.3	9.5 ± 0.3			
Na	6.33	6.6 ± 0.1	6.7 ± 0.1	6.5 ± 0.1	6.6 ± 0.2	6.8 ± 0.1	6.1	6.4
Mg	7.58	6.5 ± 0.4	6.6 ± 0.4	6.3 : ±0.4	6.3 : ±0.4	6.5 ± 0.3	6.4	6.2
Al	6.47	6.5 ± 0.2	6.6 ± 0.2	6.5 ± 0.3	6.6 ± 0.3	6.3	6.0	5.7
Si	7.55	7.3 ± 0.0	7.1 ± 0.2	7.1 ± 0.2	7.1 ± 0.0	7.5 ± 0.2	7.1	7.0
P	5.45	6.2	6.2 ± 0.4	6.1 ± 0.4	6.3			
S	7.33	6.8 ± 0.1	6.6 ± 0.1	6.5 ± 0.2	6.7 ± 0.1	6.9 ± 0.1	6.9	6.4
K	5.12		4.9 ± 0.0	4.7	5.0 ± 0.1	5.0 ± 0.0		
Ca	6.36	5.2 ± 0.1	5.6 ± 0.3	5.4 ± 0.3	5.6 ± 0.4	5.5 ± 0.4	5.4	5.1
Sc	3.17	3.1 ± 0.1	3.1 ± 0.1	3.2 ± 0.1	3.3 ± 0.2	3.9 ± 0.2		2.9
Ti	5.02	4.0 ± 0.1	4.1 ± 0.2	4.2 ± 0.2	4.4 ± 0.2	4.6 ± 0.2		4.1
Cr	5.67	4.5 ± 0.1	4.5 ± 0.2	4.7 ± 0.2	4.8 ± 0.2	5.1 ± 0.2		4.2
Fe	7.50	6.4 ± 0.2	6.4 ± 0.2	6.4 ± 0.2	6.6 ± 0.2	6.6 ± 0.3	6.5	6.0
Ni	6.25	6.1 ± 0.3	6.1 ± 0.4	5.9 ± 0.2	6.0 ± 0.2	6.2 ± 0.2	5.9	5.9
Cu	4.21		5.0 ± 0.3	5.0 ± 0.2	5.1 ± 0.0	5.0 ± 0.1		
Zn	4.60	4.9 ± 0.2	4.8 ± 0.2	4.9	5.1	5.4	4.3	4.4
Rb	2.60		< 3.7	4.2		4.6		
Sr	2.97	4.7 : ±0.1	4.9 : ±0.2	5.0 : ±0.4		5.4 : ±0.0		2.2
Y	2.24	3.2 ± 0.3	3.3 ± 0.3	3.3 ± 0.3	3.7 ± 0.2	4.2 ± 0.2	2.1	2.2
Zr	2.60	3.0 ± 0.2	3.0 ± 0.3	3.2 ± 0.2	3.3 ± 0.2	3.5 ± 0.3		2.1
Ba	2.13	1.5 ± 0.1	1.5 ± 0.2	1.5 ± 0.2	1.8 ± 0.1	1.9 ± 0.4	1.6	1.3
La	1.17		< 1.6		1.3	1.5		0.4

Asplund et al 1999

Observational constraints: Ratio of heavy ($hs = \langle \text{Ba, La} \rangle$) to light s-process elements ($ls = \langle \text{Rb, Sr, Y, Zr} \rangle$) is very low (Asplund et al. 1999). Other observed abundances (e.g. Li, P, Cu, Zn up and S, Ti, Cr and Fe down) are also **anomalous in a way that can not be reconciled with any known s-process production site during the progenitor AGB evolution** (Busso et al. 2001). In particular, no or very few neutrons would be released in the **early-split convection scenario predicted from stellar evolution**.



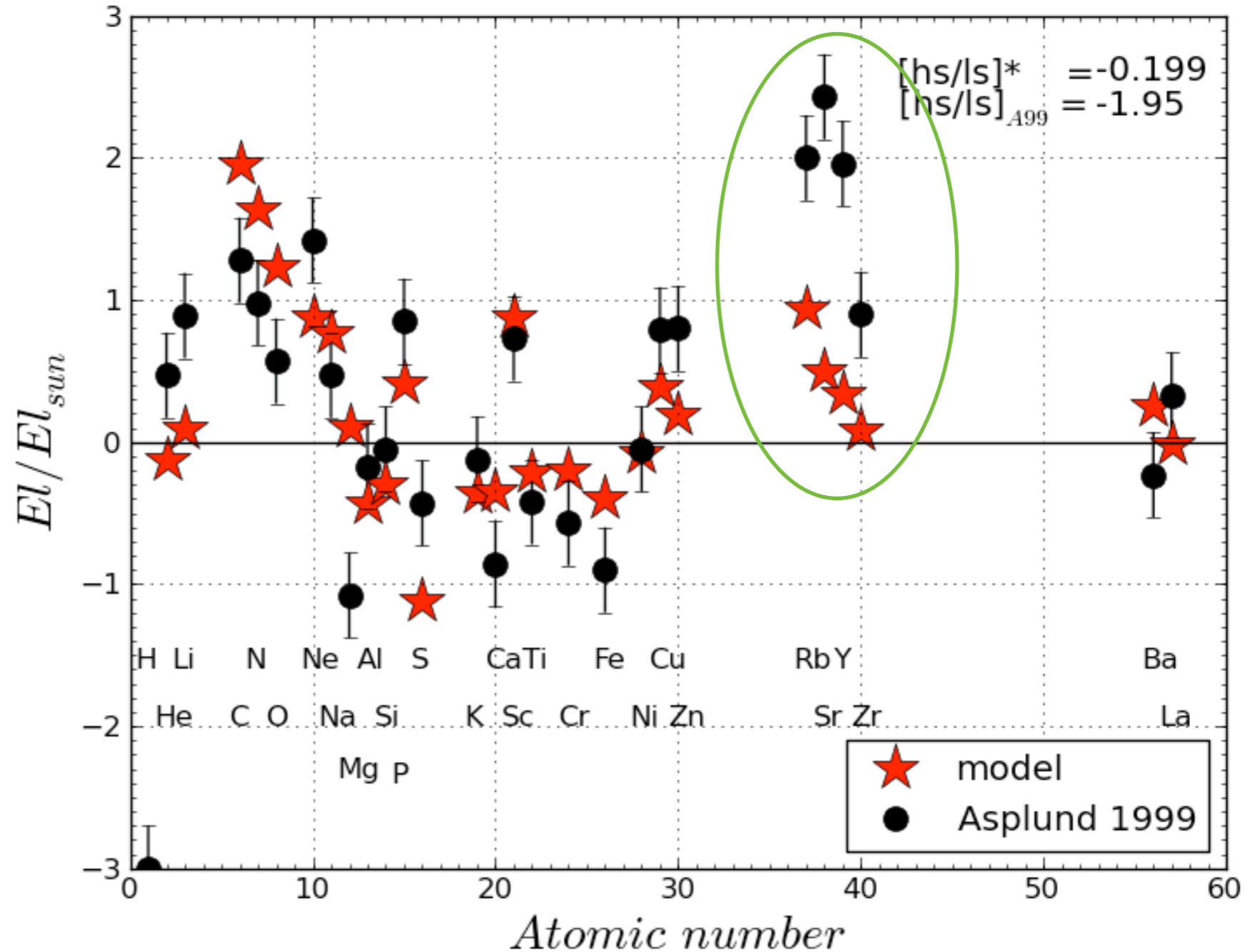
Stellar evolution picture of the HIF in Sakurai's object



Stellar evolution predictions for the nuclear combustion in Sakurai's object: Convective diffusion coefficient and H abundance profile at the beginning of the H-ingestion flash (t_0) and at the time when the split of the convection zone appears at $t_1 = t_0 + 8.58 \cdot 10^5 \text{s}$. In our 1D models mixing through this split is not possible. **Left panel:** the outer section of the convection zone showing the location of the split as a deep dip in D ; **right panel:** just the interface of the outer boundary of the convection zone.

Abundance distribution according to stellar evolution mixing

Can not reproduce observed abundance pattern



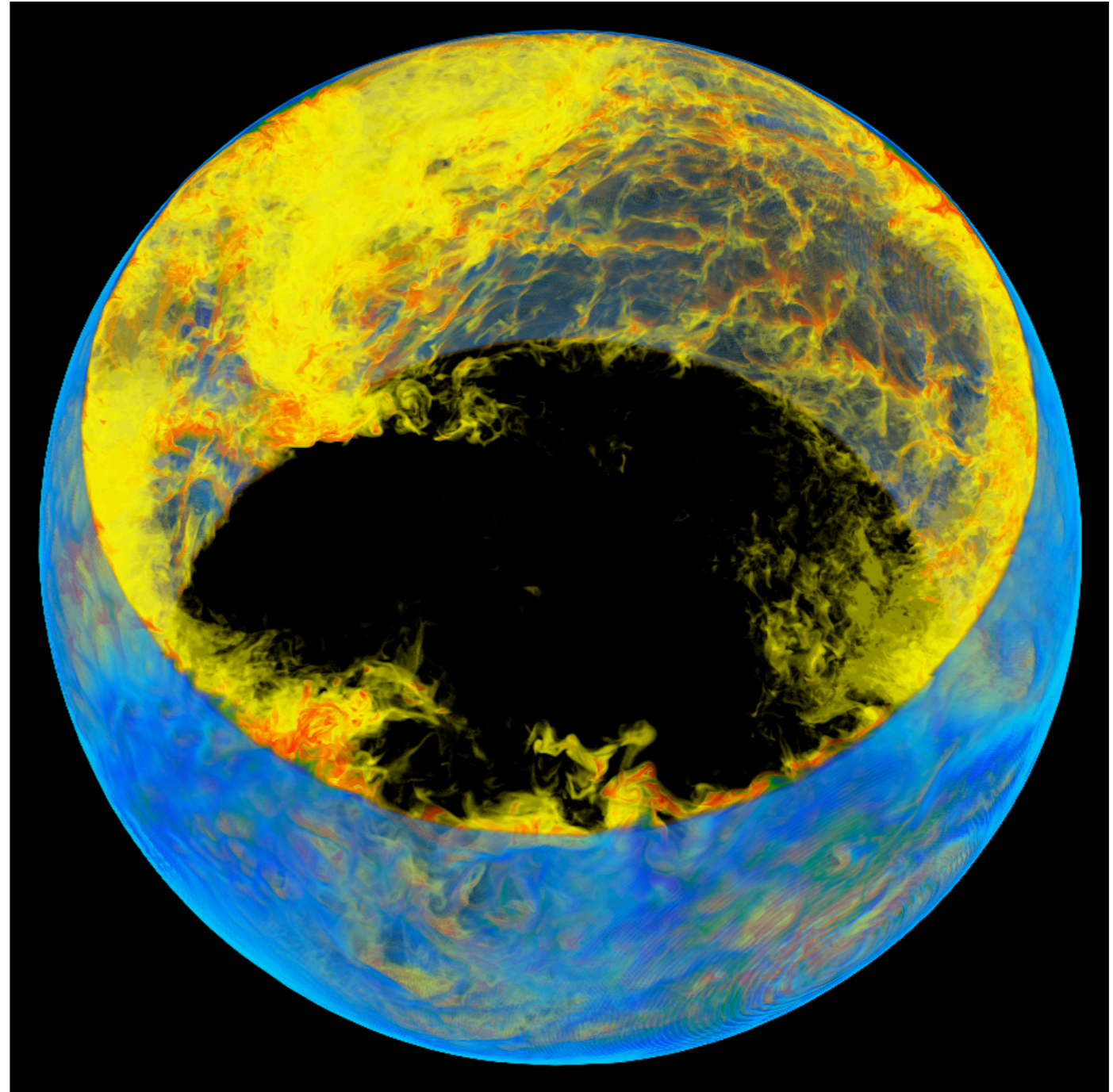
Herwig et al 2011, ApJ

Multi-dimensional stars

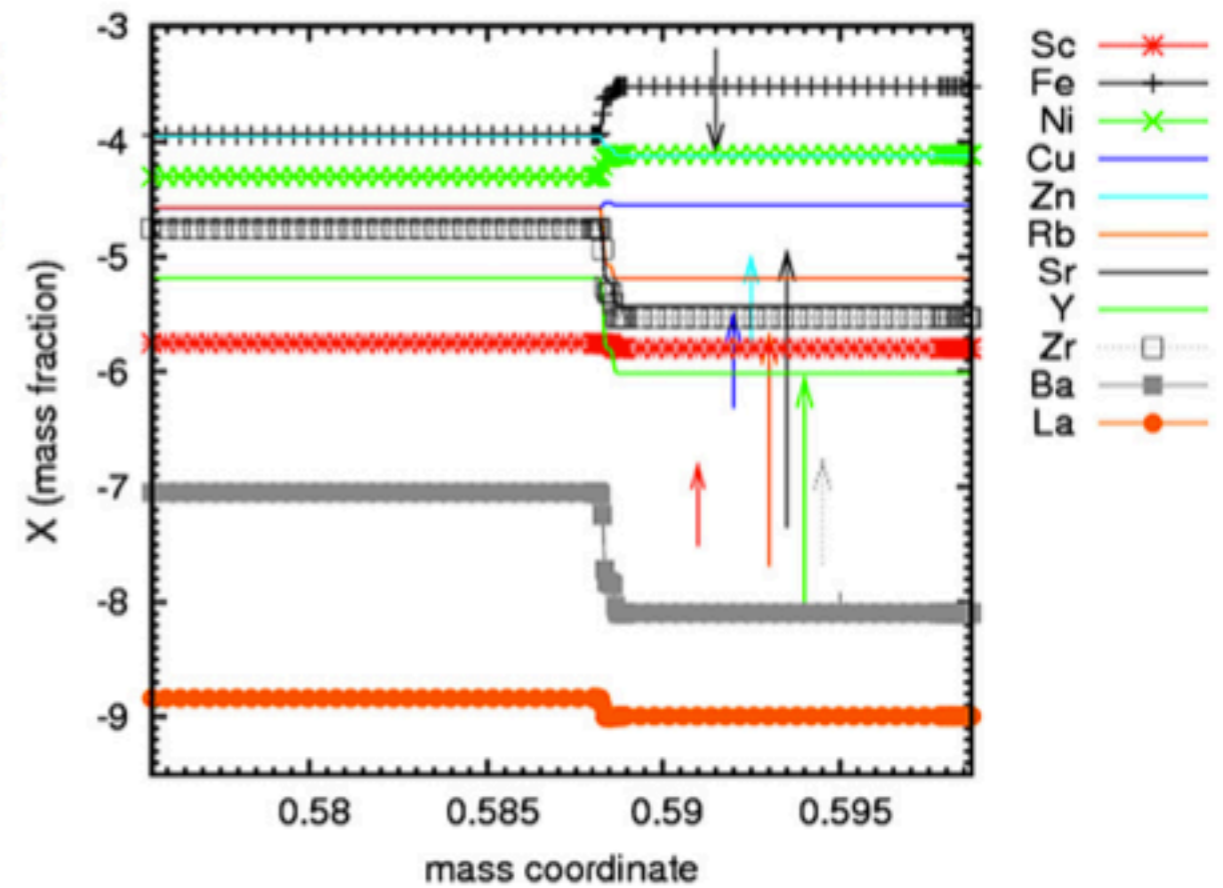
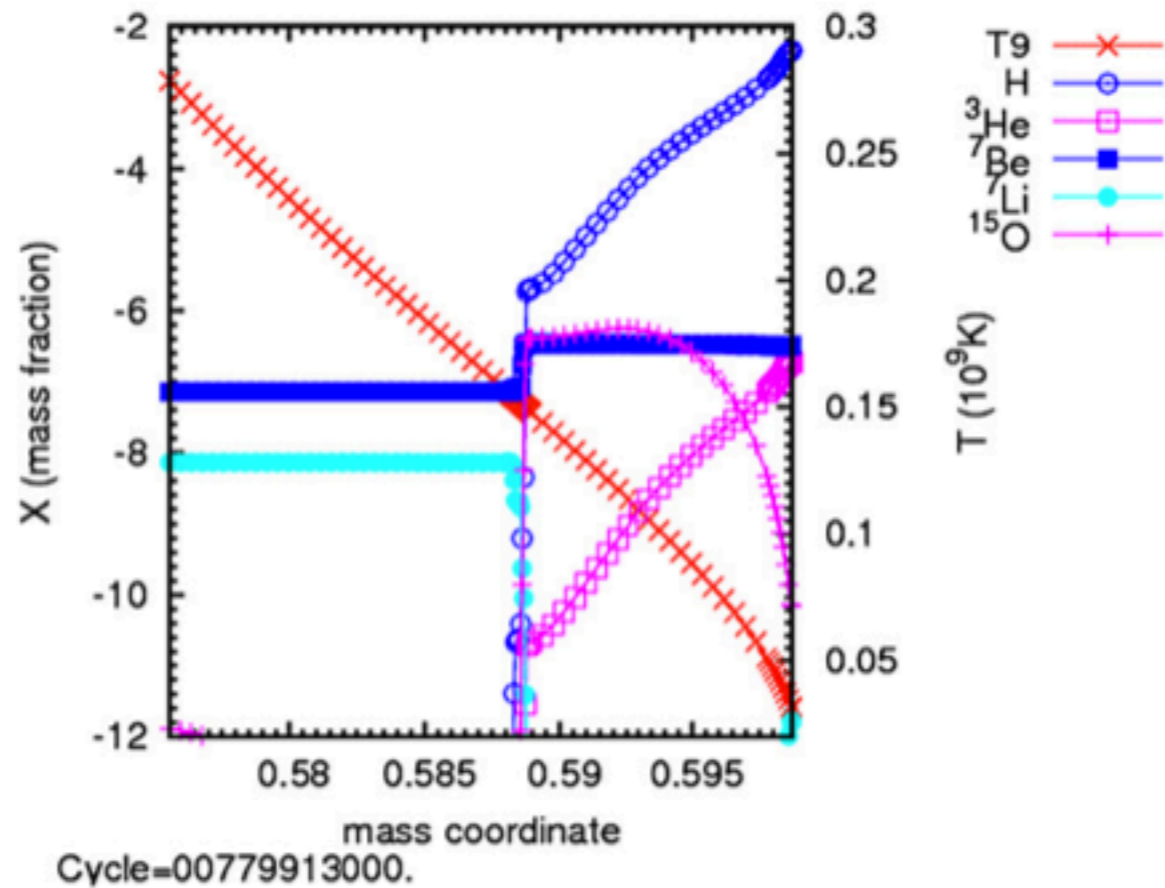
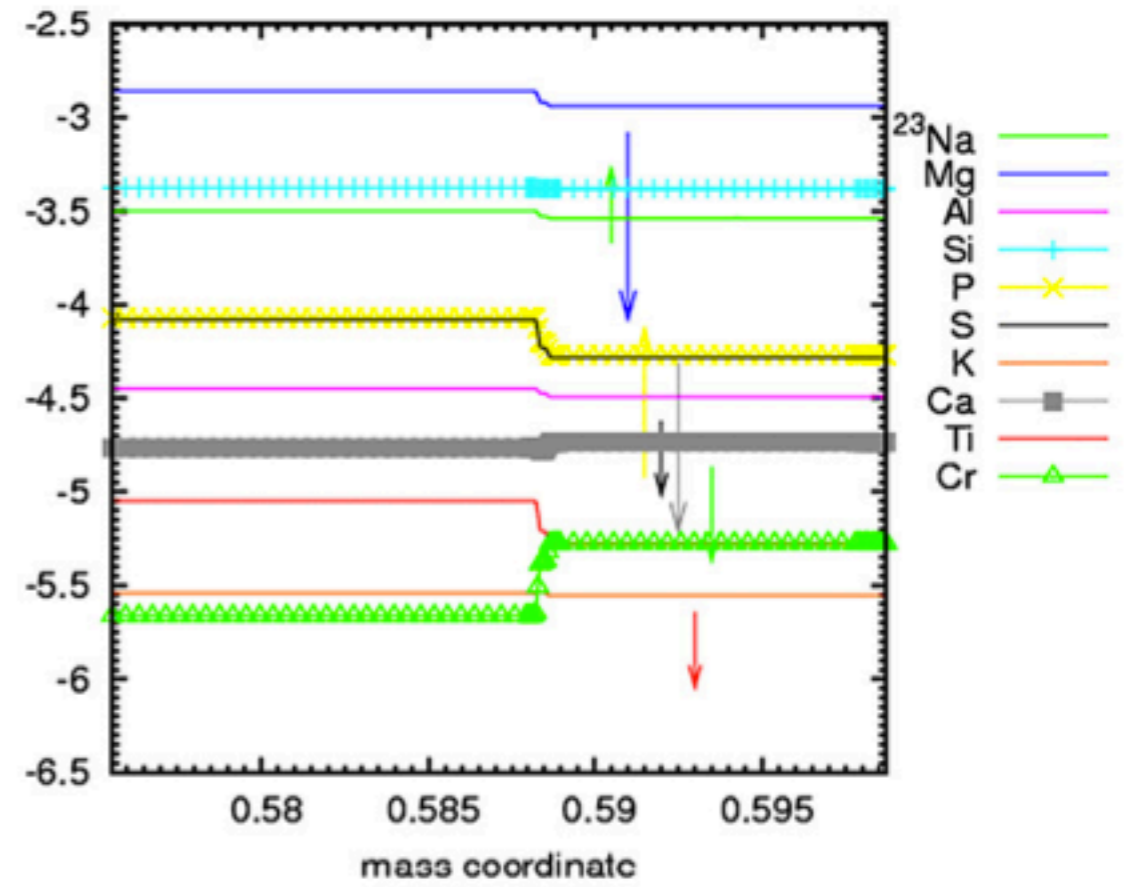
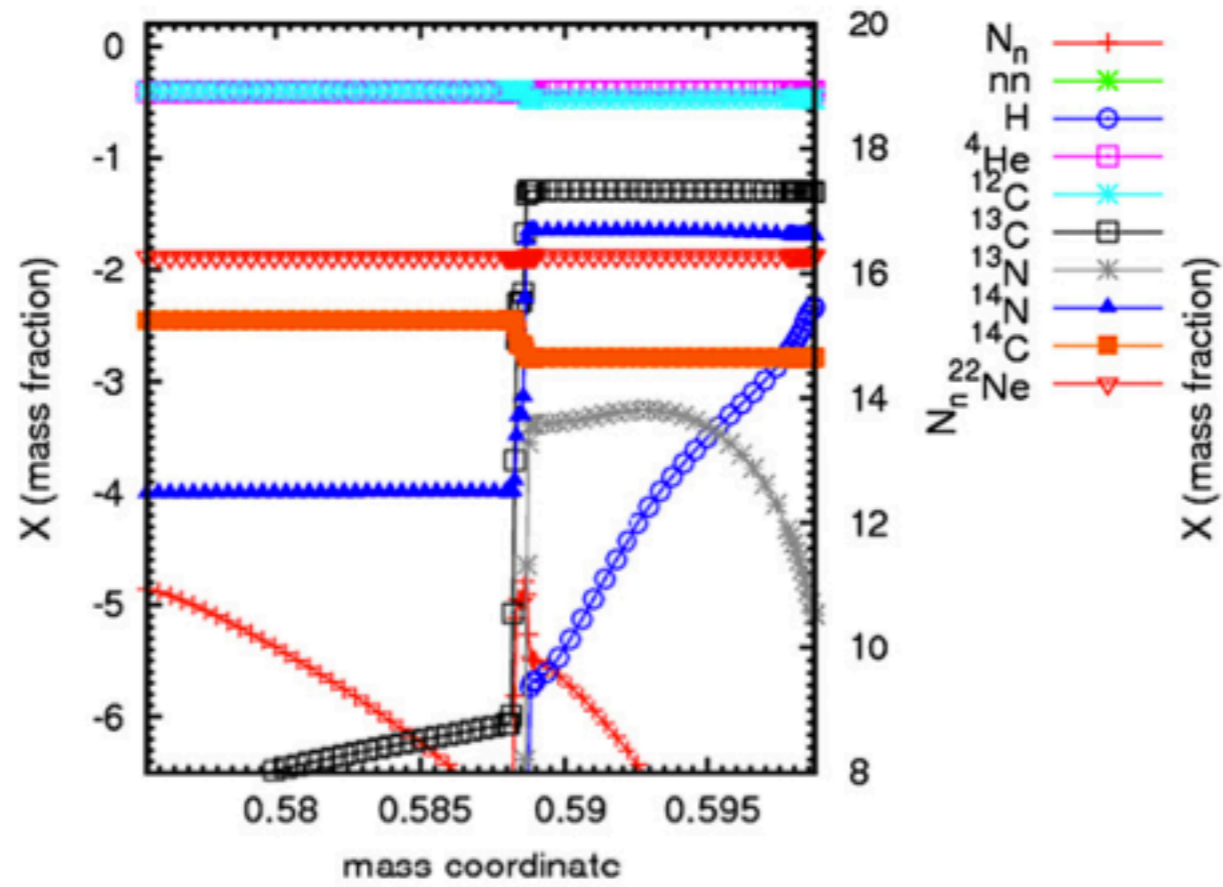
abundance of H-rich material entrained from above
into convection zone at $\sim 20ks$

Next generation He-shell flash
convection

- i. 3D 4π star-in-a-box
simulations (e.g. Herwig et al
2010, arXiv:1002.2241)
- ii. compressible gas dynamics
PPM code Paul Woodward
(<http://www.lcse.umn.edu>)
- iii. high accuracy PPB advection
scheme
- iv. 2 fluids, with individual,
realistic material densities
- v. 576^3 cartesian grid, simulated
time total 60ks
- vi. $Ma \sim 0.03$, $11H_p$ in conv.
zone



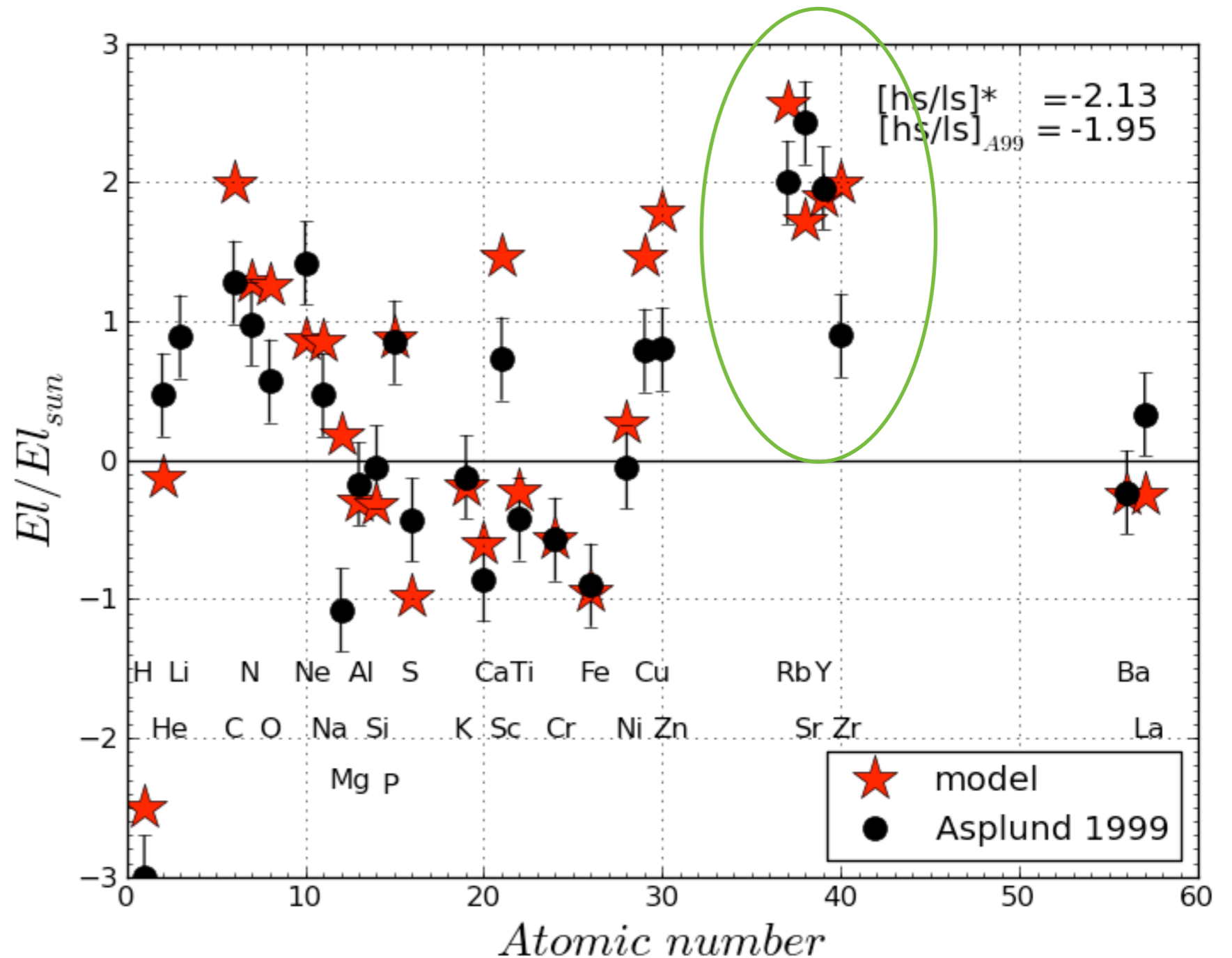
<http://www.lcse.umn.edu/index.php?c=movies>



Herwig etal 2011, ApJ

Abundance distribution according to delayed split assumption

Most abundance patterns, including low $[hs/ls]$ can be reproduced.

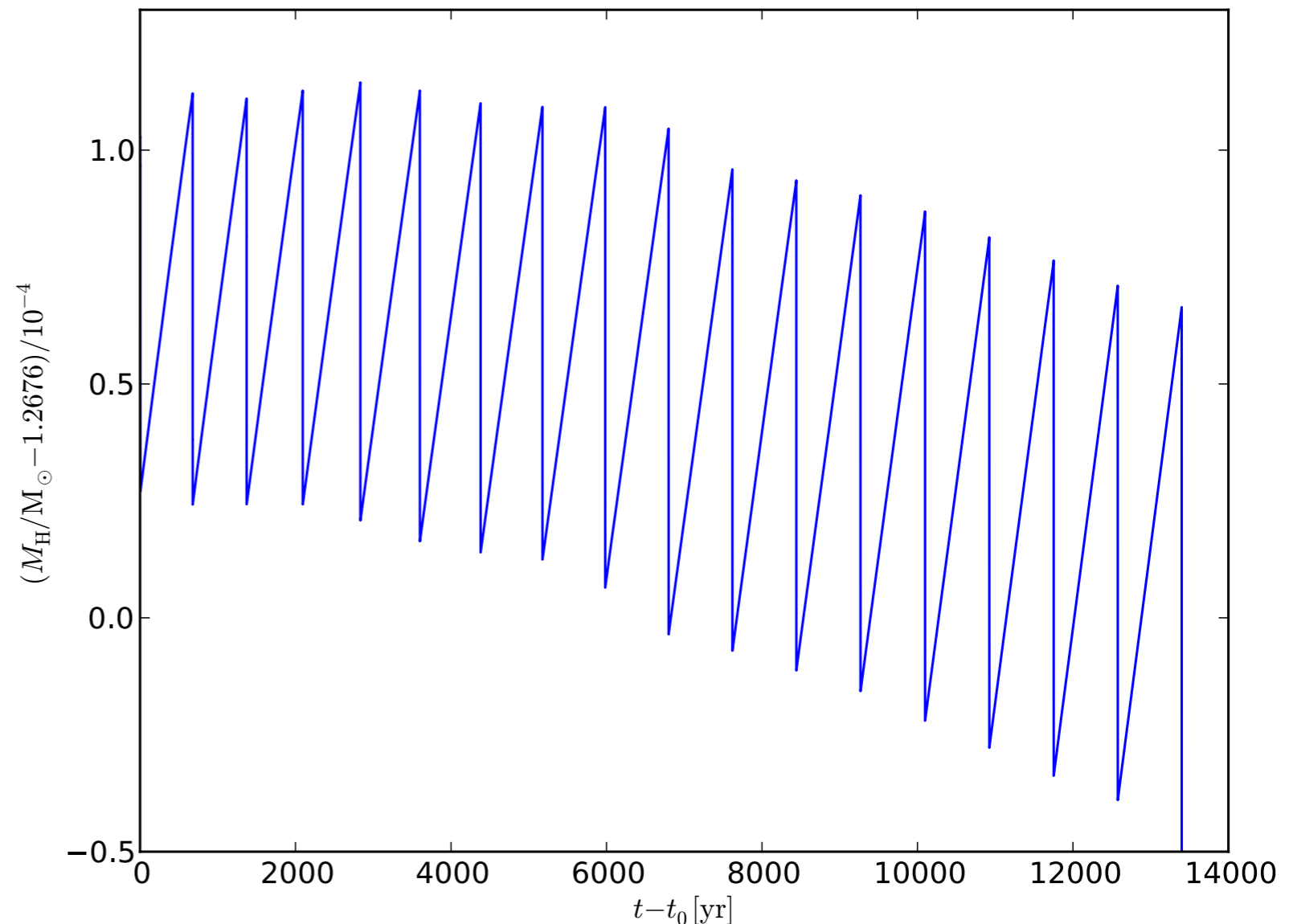


For full details see: Herwig et al 2010, arXiv:1002.2241

Super-AGB star models at low metallicity

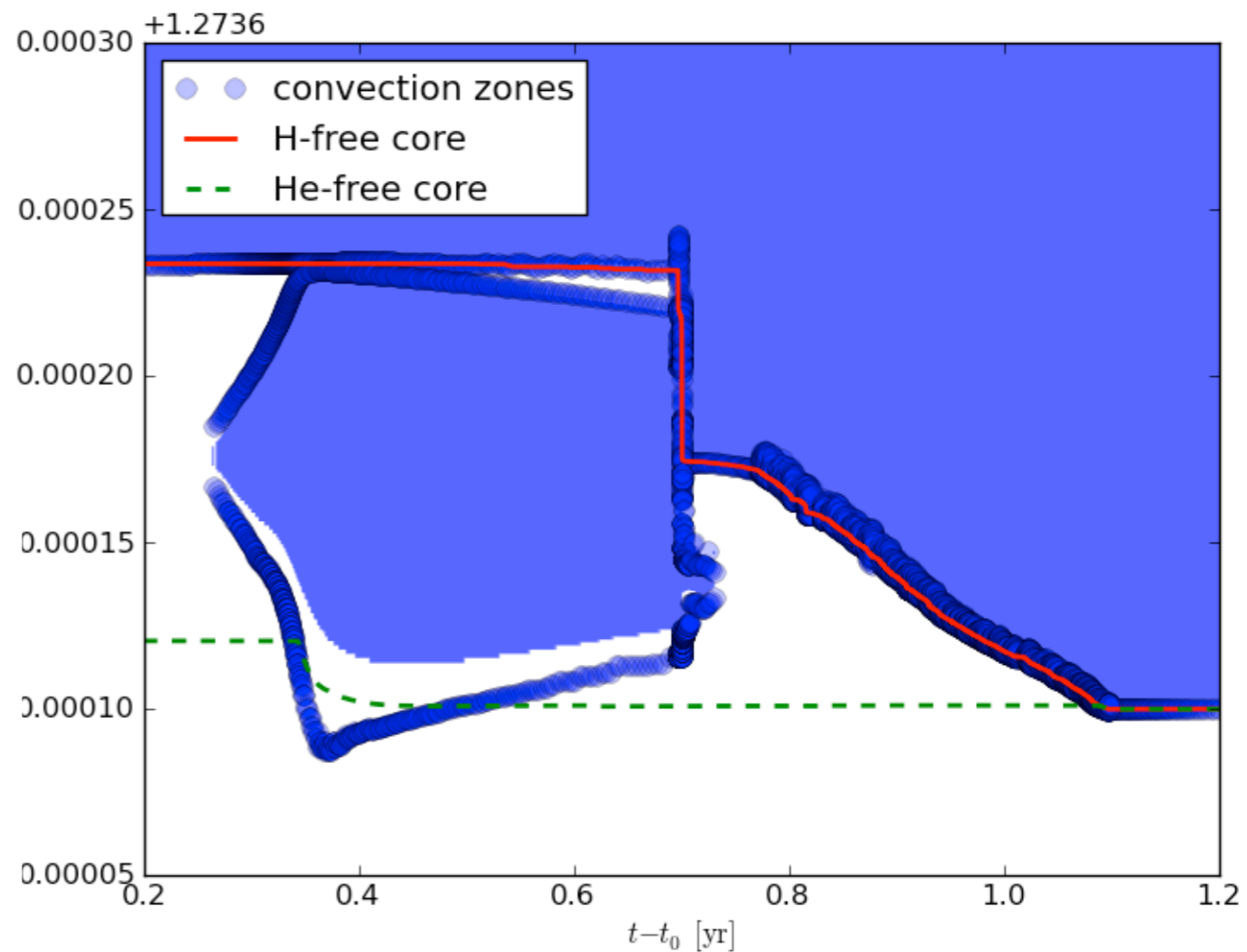
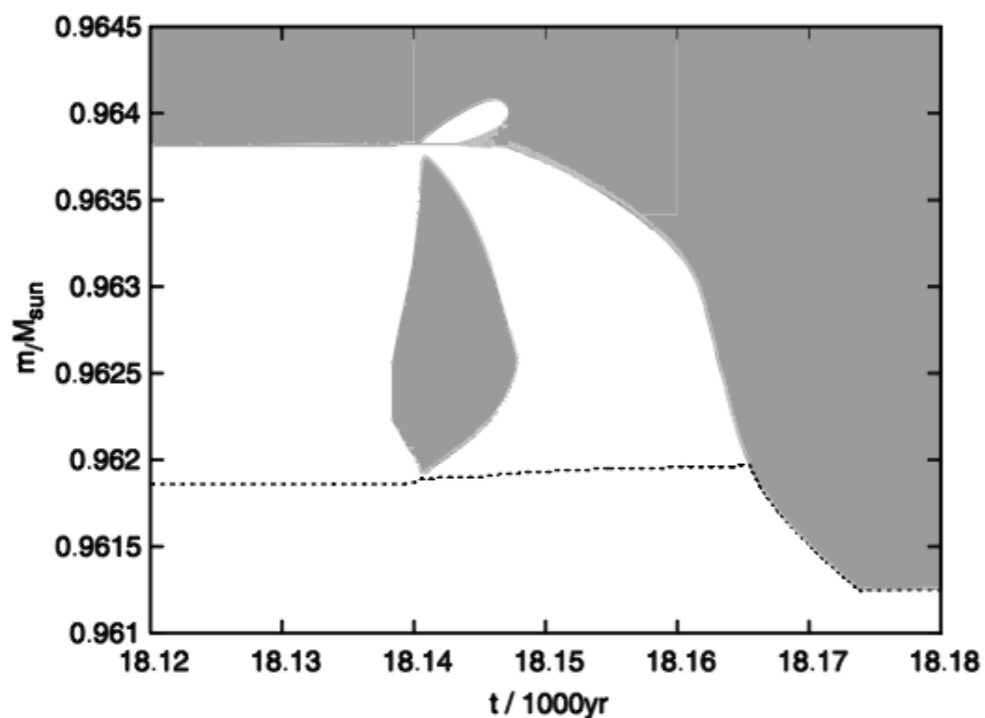
- * stellar evolution (with MESA), $M_{\text{ini}}=7M_{\odot}$
- * $[\text{Fe}/\text{H}]=-1.7$, α -enhanced initial abundance 1st, 2nd dredge-ups, 'dredge-out' \rightarrow CNO abundance env. 1st TP $\odot - 0.5\text{dex}$
- * convective boundary mixing (tiny: $f=0.002/0.004$)

Healthy thermal pulses with 3rd dredge-up



H-combustion in super-AGB star models

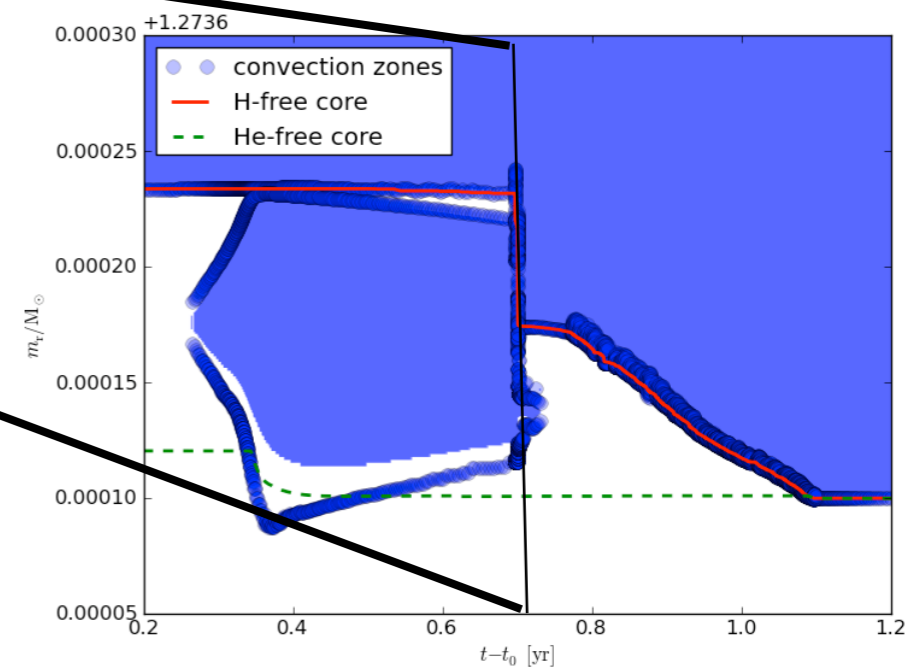
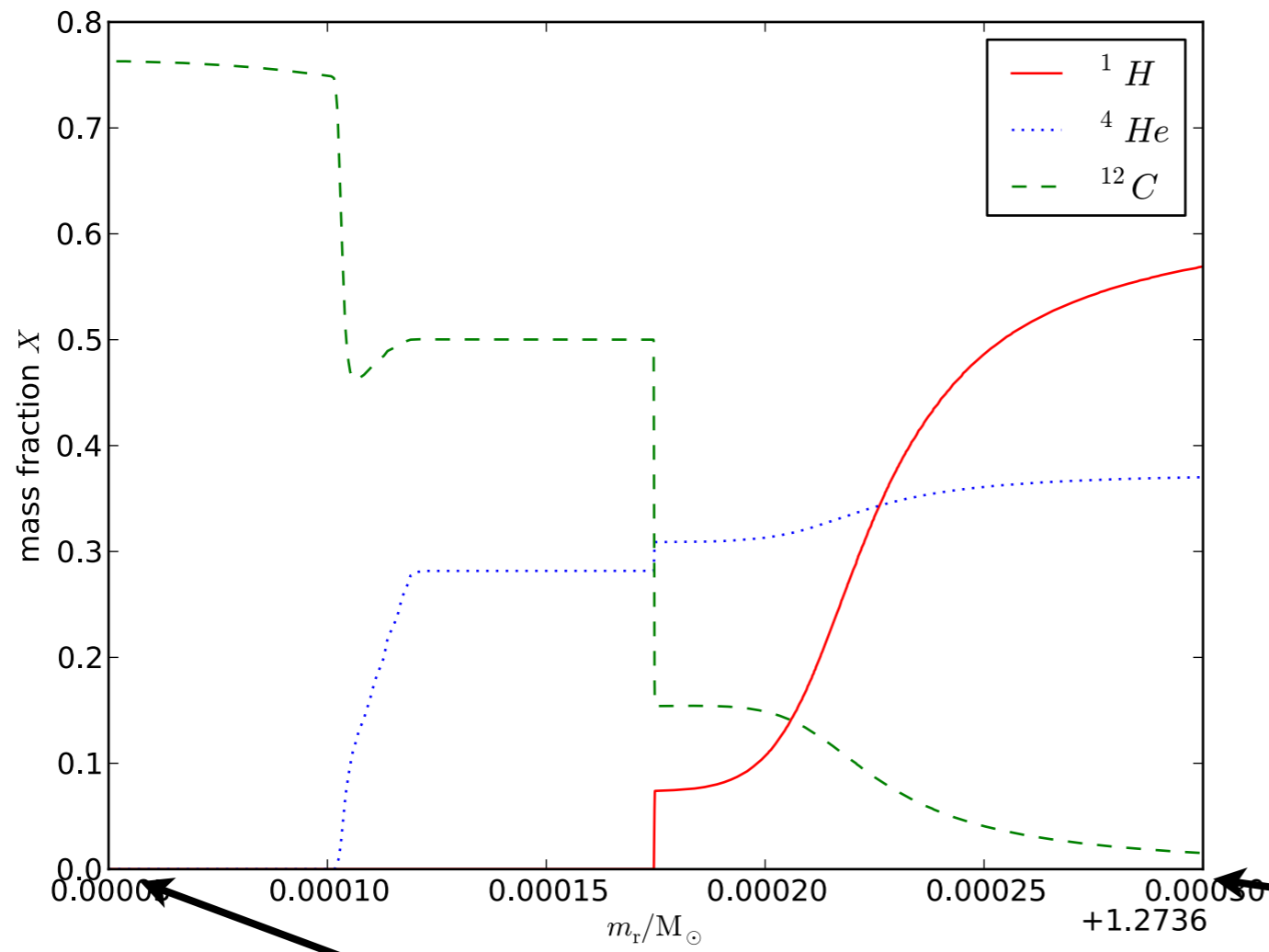
- * hot dredge-up with H-mixing into still live He-shell flash convection zone
- * H-burning $L_{\text{peak}} \sim 10^9 L_{\odot}$
- * recurrent! followed after all of the



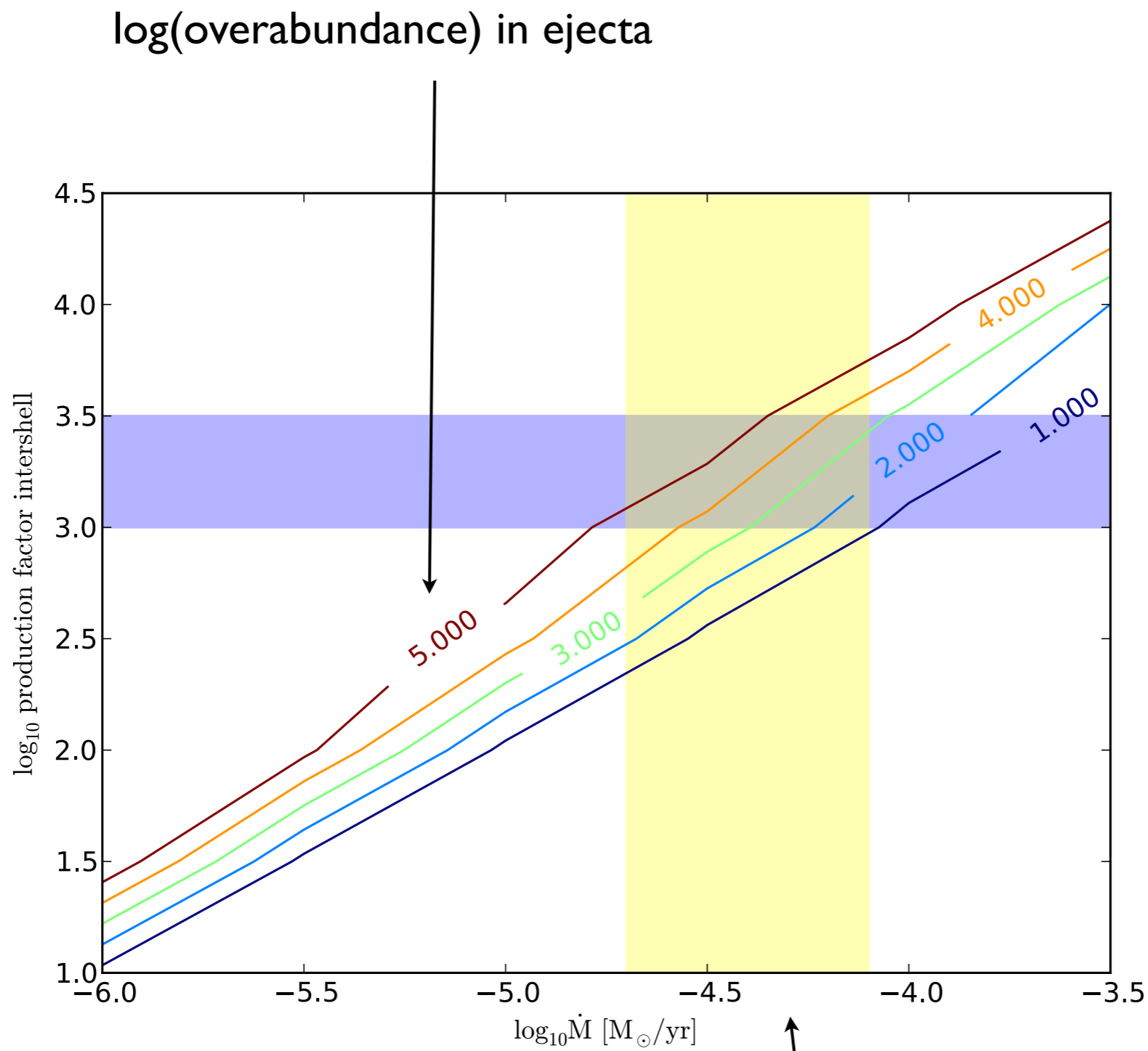
Herwig et al. submitted

$5M_{\odot}$, $[\text{Fe}/\text{H}] = -2/3$,
Herwig 2004

Abundance profile in burn/mix H-combustion layer



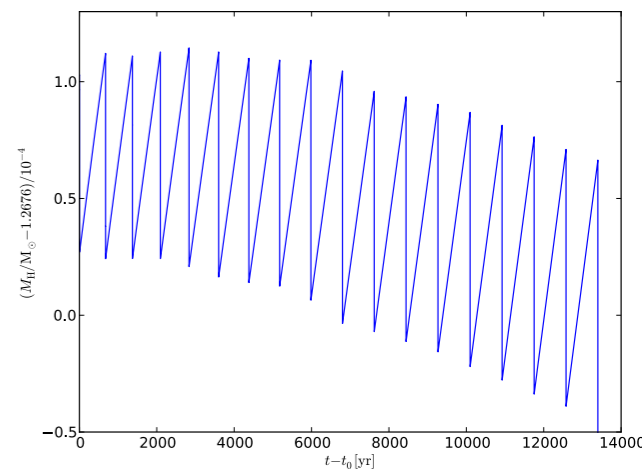
Mix- and envelope-enrichment model



range of mass loss for luminous M-type giants (van Loon et al. 2005)

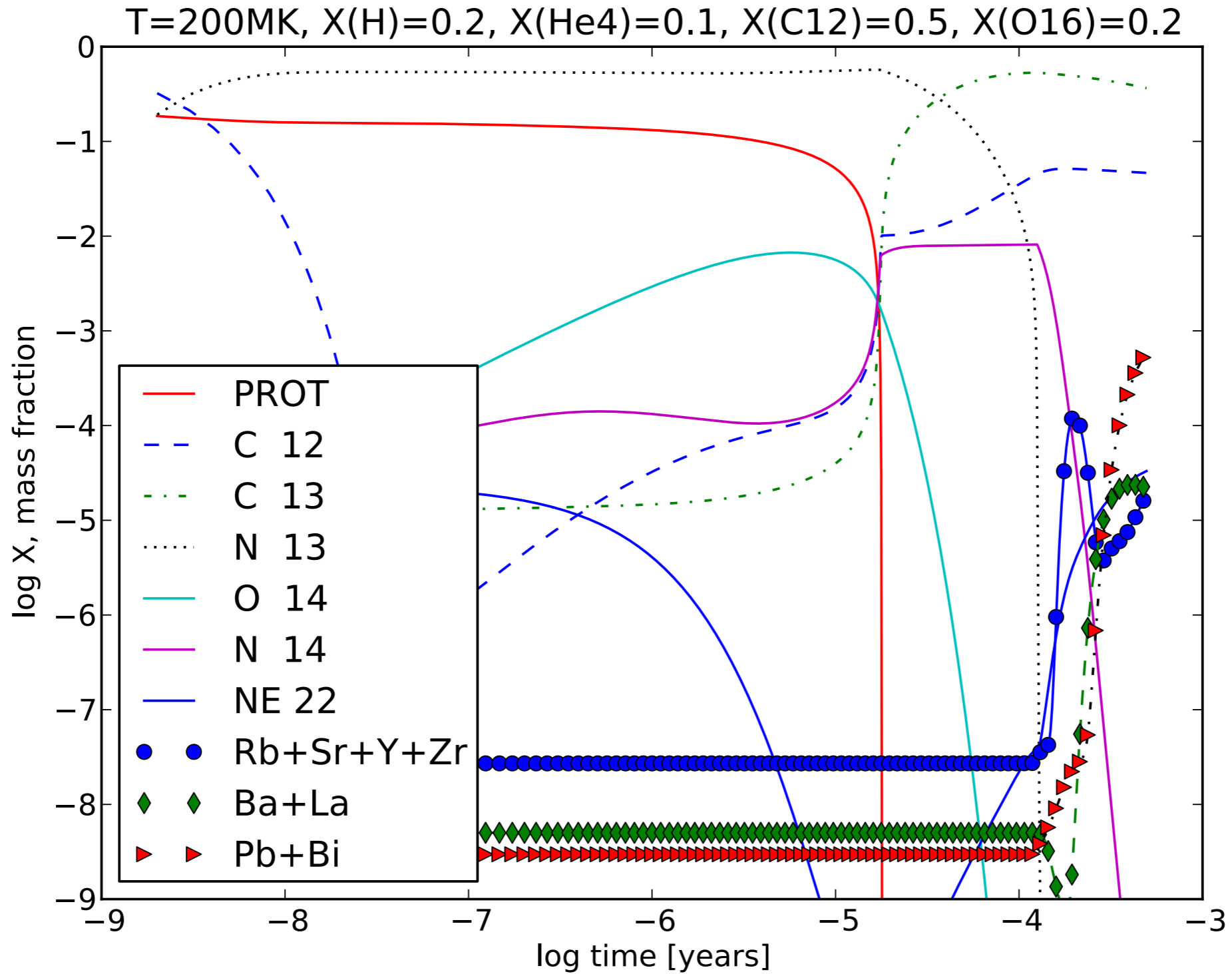
$\log(\dot{M}) = -5$ (-4) \Rightarrow
800 (80) TPs

total mass



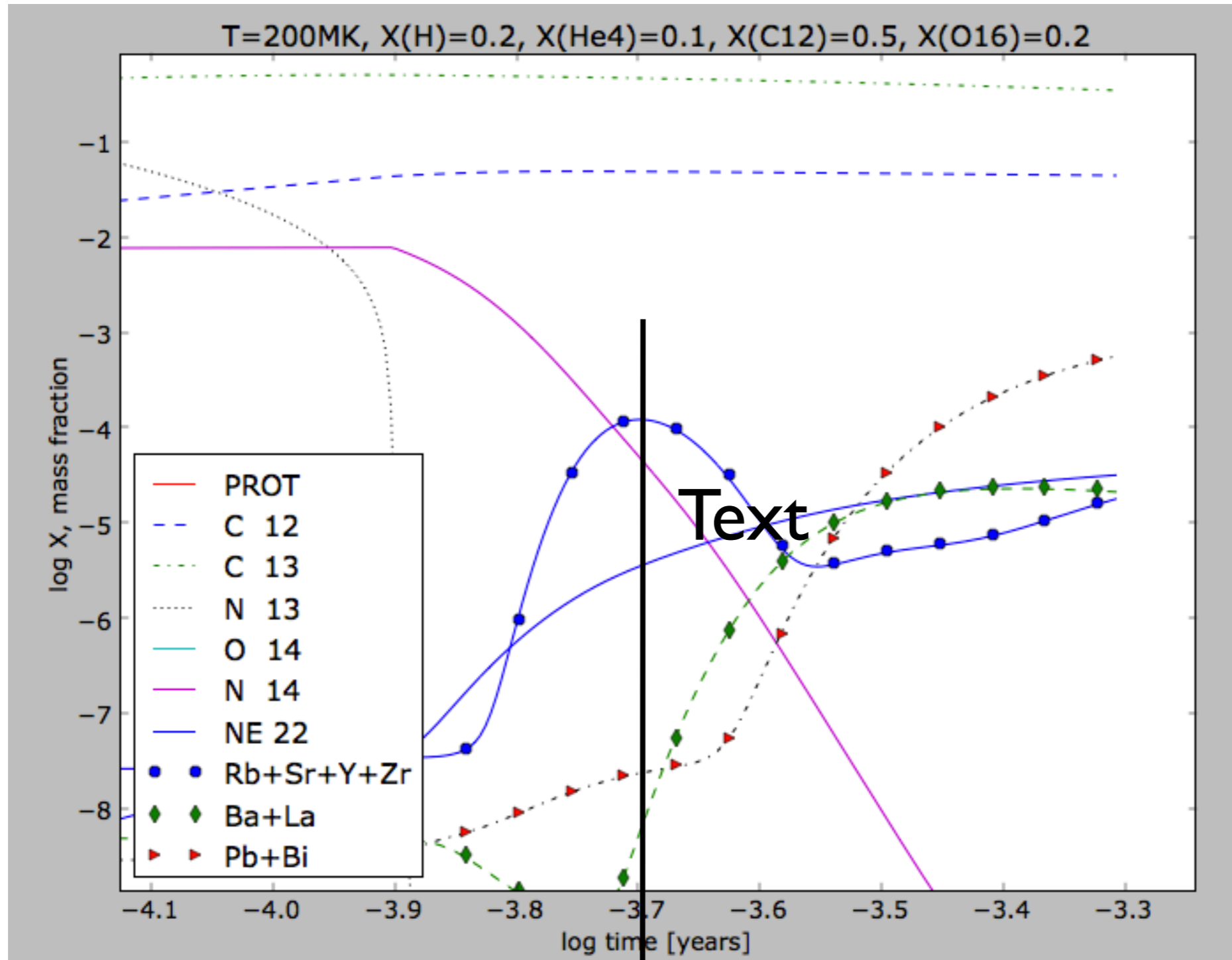
Herwig et al. submitted

One-zone nucleosynthesis of H-combustion



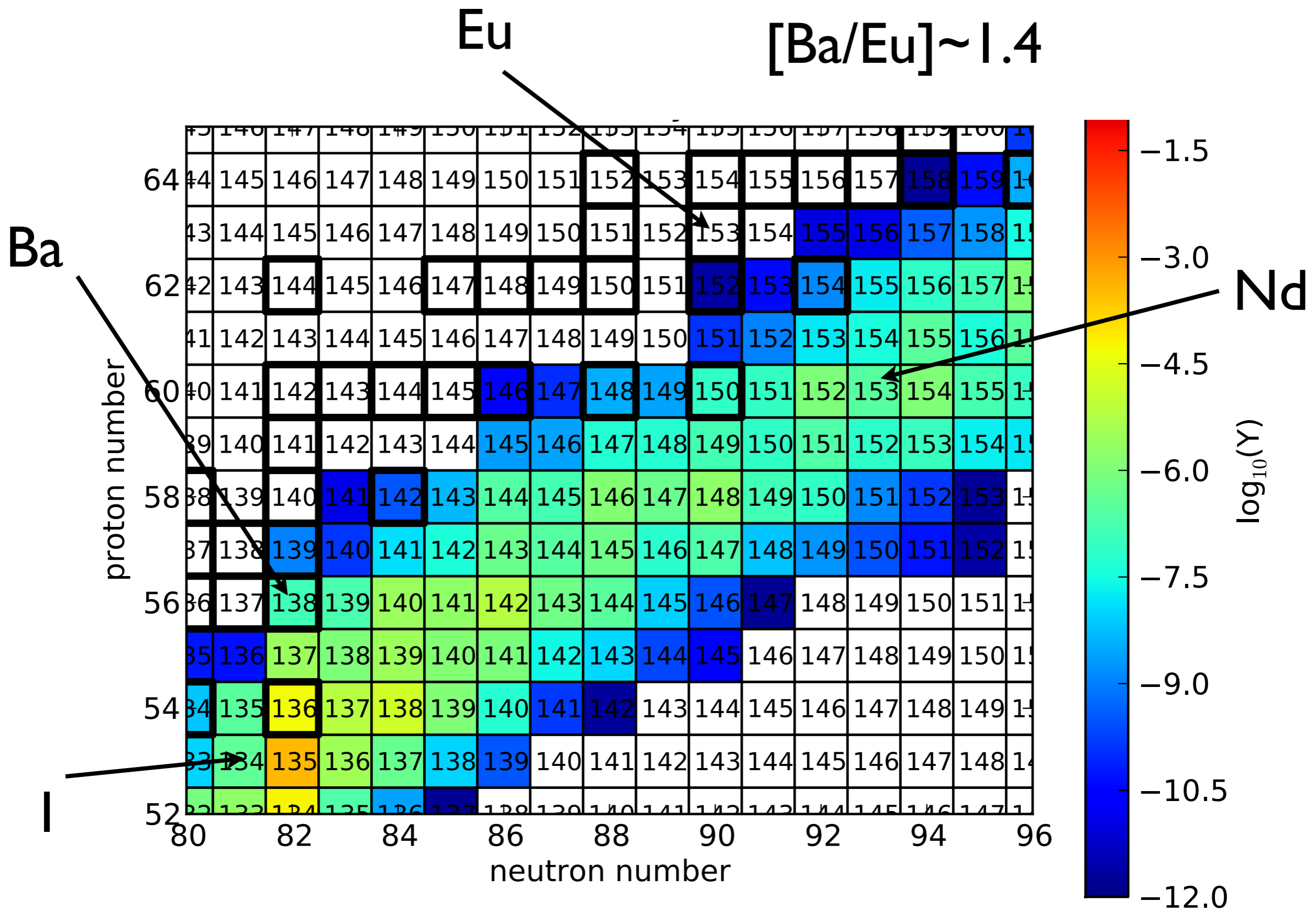
One-zone nucleosynthesis of H-combustion

H-combustion in super-AGB stars



$$N_n \sim 10^{15} \text{cm}^{-3}$$

6200s

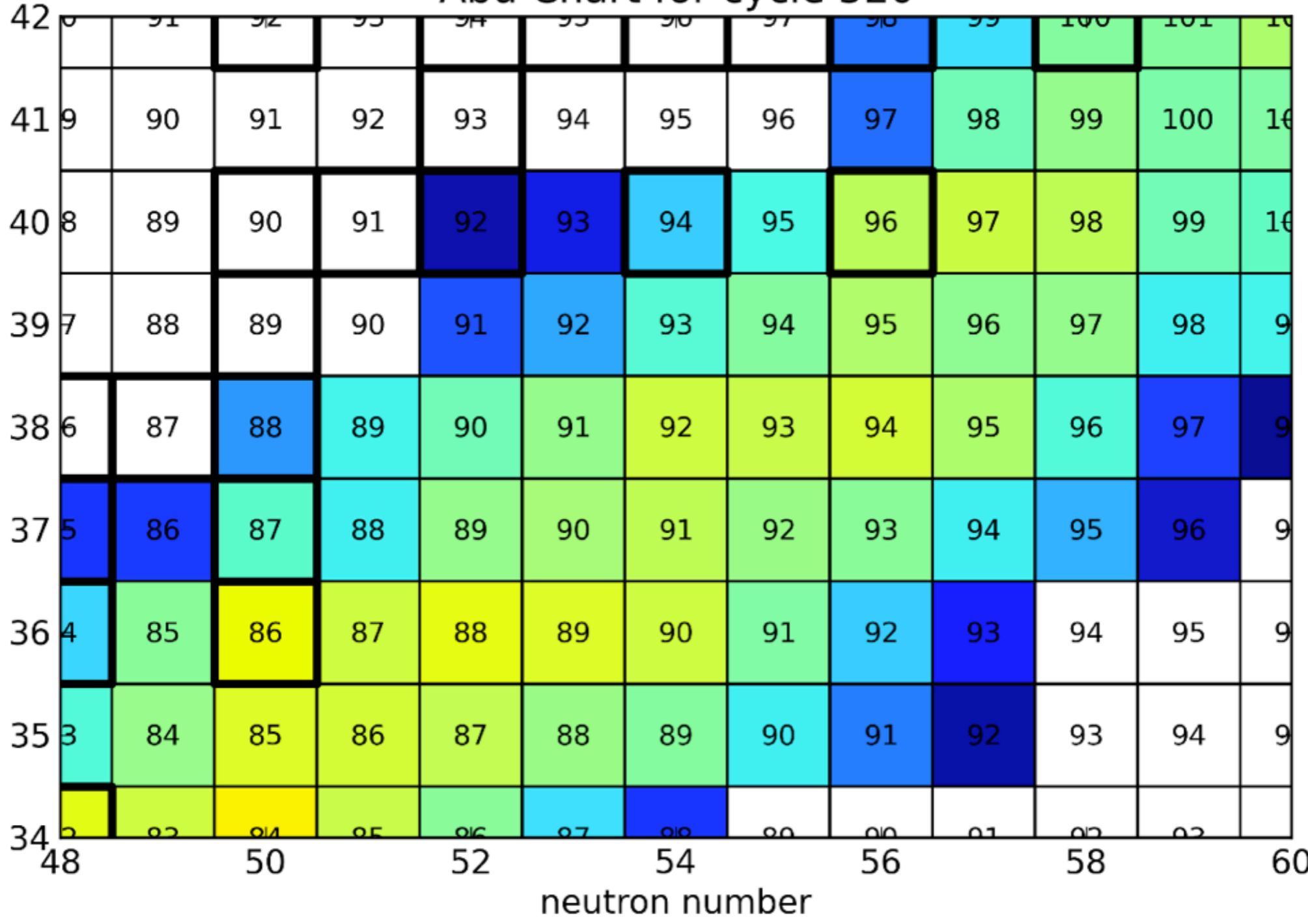




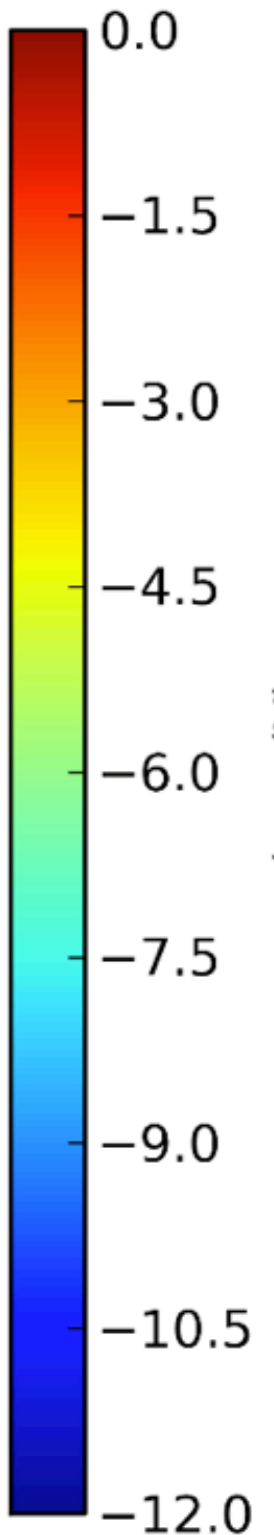
Abu Chart for cycle 520

Zr
Y
Sr
Rb

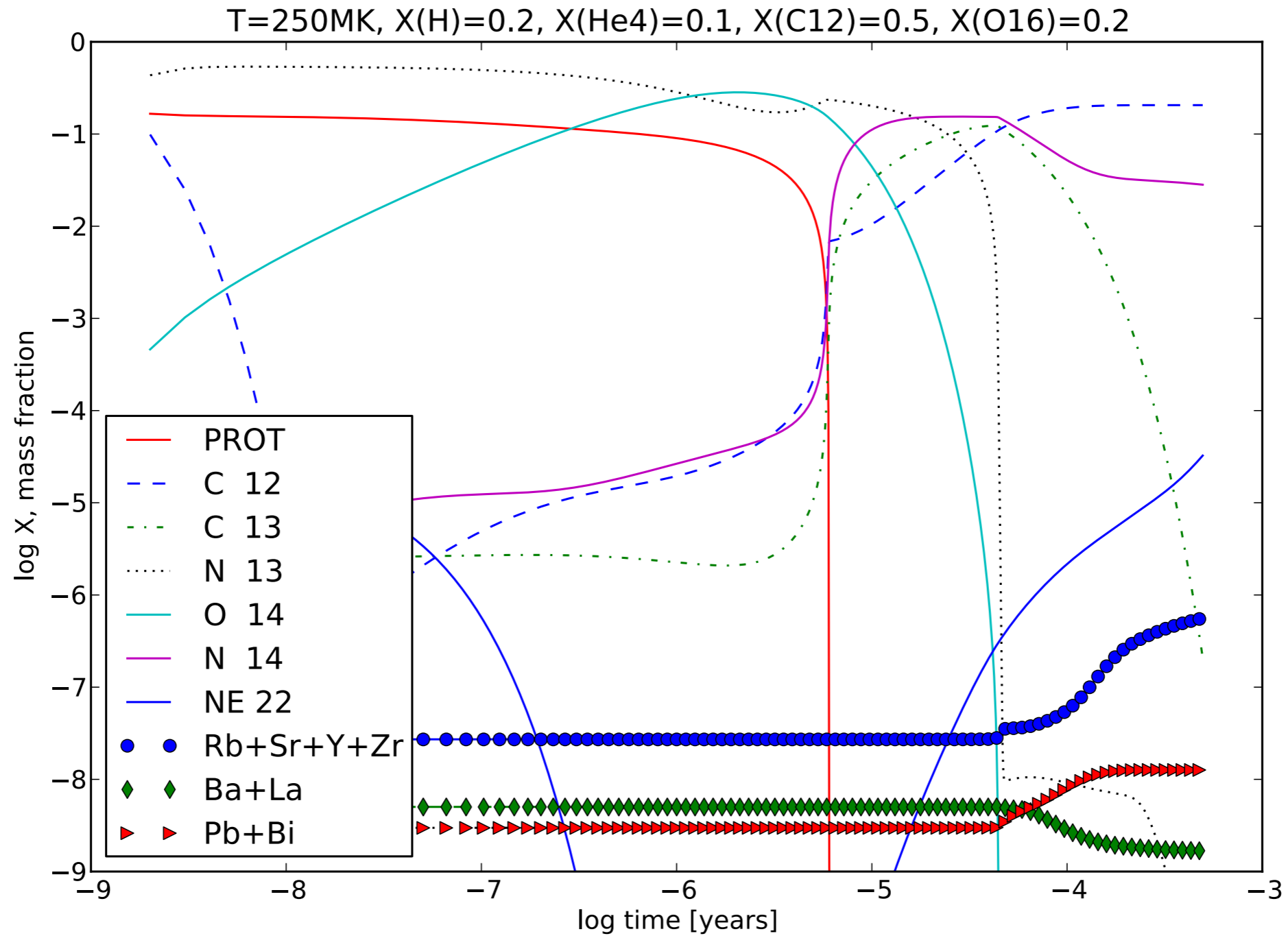
proton number



log₁₀(Y)



One-zone nucleosynthesis of H-combustion





Conclusions

H-combustion is

- n-capture conditions between s and r
- non-standard
- has been shown to result in excess first peak production in Sakurai's object
- shows in a wide range of low-metallicity environments, including possibly the super-AGB stars
- combustion events may very well show a spread, including leaking into second or third peak in some cases

→ possible contribution to (low-Z) LEPP